



National Library
of Canada

Canadian Theses Service

Ottawa, Canada
K1A 0N4

Bibliothèque nationale
du Canada

Service des thèses canadiennes

NOTICE

The quality of this microform is heavily dependent upon the quality of the original thesis submitted for microfilming. Every effort has been made to ensure the highest quality of reproduction possible.

If pages are missing, contact the university which granted the degree.

Some pages may have indistinct print especially if the original pages were typed with a poor typewriter ribbon or if the university sent us an inferior photocopy.

Reproduction in full or in part of this microform is governed by the Canadian Copyright Act, R.S.C. 1970, c. C-30, and subsequent amendments.

AVIS

La qualité de cette microforme dépend grandement de la qualité de la thèse soumise au microfilmage. Nous avons tout fait pour assurer une qualité supérieure de reproduction.

S'il manque des pages, veuillez communiquer avec l'université qui a conféré le grade.

La qualité d'impression de certaines pages peut laisser à désirer, surtout si les pages originales ont été dactylographiées à l'aide d'un ruban usé ou si l'université nous a fait parvenir une photocopie de qualité inférieure.

La reproduction, même partielle, de cette microforme est soumise à la Loi canadienne sur le droit d'auteur, SRC 1970, c. C-30, et ses amendements subséquents.

ROLE FOR THE PERICYTE IN A MODEL OF INFLAMMATION: AN ELECTRON
MICROSCOPIC STUDY OF THE VENULE WALL

A Thesis
Submitted to the Graduate Faculty
in Partial Fulfillment of the Requirements
for the Degree of
Master of Science
in the Department of Anatomy and Physiology
Faculty of Veterinary Medicine
University of Prince Edward Island

Wendy T. Drake
Charlottetown, P.E.I.
August, 1989

© 1989. W.T. Drake



National Library
of Canada

Canadian Theses Service Service des thèses canadiennes

Ottawa, Canada
K1A 0N4

Bibliothèque nationale
du Canada

The author has granted an irrevocable non-exclusive licence allowing the National Library of Canada to reproduce, loan, distribute or sell copies of his/her thesis by any means and in any form or format, making this thesis available to interested persons.

The author retains ownership of the copyright in his/her thesis. Neither the thesis nor substantial extracts from it may be printed or otherwise reproduced without his/her permission.

L'auteur a accordé une licence irrévocabile et non exclusive permettant à la Bibliothèque nationale du Canada de reproduire, prêter, distribuer ou vendre des copies de sa thèse de quelque manière et sous quelque forme que ce soit pour mettre des exemplaires de cette thèse à la disposition des personnes intéressées.

L'auteur conserve la propriété du droit d'auteur qui protège sa thèse. Ni la thèse ni des extraits substantiels de celle-ci ne doivent être imprimés ou autrement reproduits sans son autorisation.

ISBN 0-315-53039-1

Canada

CONDITIONS OF USE

The author has agreed that the Library, University of Prince Edward Island, may make this thesis freely available for inspection. Moreover, the author has agreed that permission for extensive copying of this thesis for scholarly purposes may be granted by the professor or professors who supervised the thesis work recorded herein or, in their absence, by the Chairman of the Department or the Dean of the Faculty in which the thesis work was done. It is understood that due recognition will be given to the author of this thesis and to the University of Prince Edward Island in any use of the material in this thesis. Copying or publication or any other use of the thesis for financial gain without approval by the University of Prince Edward Island and the author's written permission is prohibited.

Requests for permission to copy or to make any other use of material in this thesis in whole or in part should be addressed to:

Chairman of the Department of Anatomy and Physiology

Faculty of Veterinary Medicine

University of Prince Edward Island

Charlottetown, P. E. I.

Canada

SIGNATURE PAGE(S)

iii_iv

REMOVED

ABSTRACT

Transmission electron microscopy and morphometric techniques were employed to quantitatively assess the relationship of pericytes to endothelial cells during histamine-induced vascular permeability. This work required the use of a vascular label to identify venules. Monastral Blue (MB) was selected for this study; however, discrepancies in the literature as to its properties necessitated a re-evaluation of MB as a vascular label in rats.

In this technical study halothane-anesthetized male Sprague Dawley rats (N=23) were used to 1) determine how long MB remained available in the vascular system to label leaky venules; 2) measure the MB concentration in serum over time using spectrophotometry; and 3) characterize the cardiovascular effects of MB infusion. Arterial pressure was monitored during intravenous infusion of MB (0.1 ml/kgBW of a 3% suspension in nonionic surfactant) with or without Evans Blue, an albumin label. Localized areas of leaking venules were created by injecting 30 μ l of 10^{-4} M histamine into abdominal dermis at -2, 0, 5, 7, 10 and 15 minutes with respect to the i.v. infusion of MB. Arterial pressure decreased by $30 \pm 13\%$ (mean \pm SD, $p < .0001$) 65 ± 18 seconds after MB infusion. Sites induced to leak at 10 and 15 minutes did not label with MB, although Evans Blue-labeled albumin appeared in the interstitium. Spectrophotometric analysis of rat serum revealed that elimination of MB from the vascular system was rapid with a half-life of 3.54 ± 1.9 minutes and showed first order kinetics. MB meets the needs of light and electron microscopic study but its rapid removal from the circulation by the mononuclear phagocytic system and its effect on blood pressure must be considered when utilizing MB in experiments.

The ultrastructure of the venule wall was examined in the second experiment to 1) determine the pericyte-endothelial cell relationship in venules of three vascular beds (trachea, dermis and cremaster muscle); 2) establish whether the pericyte coverage was the same in these different anatomical locations; 3) compare separate venule wall thicknesses; and 4) determine whether pericyte coverage of endothelial gaps and junctions is random. Halothane-anesthetized male Sprague Dawley rats (N=5) received an i.v. infusion of MB followed by injection of 30 μ l of 10^{-4} histamine into the tracheal mucosa, abdominal dermis and cremaster muscle. These tissues were fixed 4 minutes later by vascular perfusion. A variety of ultrastructural changes could be detected on the venule wall of the three tissues studied. MB accumulation under pericytes, platelet adherence, endothelial gap formation and neutrophil diapedesis were evidence of an acute inflammatory response. The mean percent coverages (\pm SD) of the venule wall by pericytes were: trachea 82 ± 12 , dermis 71 ± 20 and

cremaster 85 ± 18 . There was a significant difference in coverage between dermis and cremaster muscle venules ($p=.0083$). There was no significant difference between mean vessel wall thicknesses (\pm SD) in the three tissues: trachea 1.68 ± 0.92 (μm), dermis 1.74 ± 0.82 and cremaster 1.97 ± 0.77 . Chi-square analysis indicated that pericytes are concentrated over endothelial cell gaps that occur in response to histamine in cremaster muscle venules. Pericytes are also concentrated over endothelial cell junctions in dermis and cremaster muscle venules. These results therefore suggest a role for the pericyte in junction-related aspects of venule function in rat dermis and cremaster venules. Possible roles include providing physical protection of junctions and sites of gap formation, and blocking or delaying extravasation of vascular label, platelets and erythrocytes. The physical protection of the vessel wall is especially apparent during diapedesis.

DEDICATION

To my son, Justin Ford Drake

Somedays I feel I'm missing seeing you grow, but I remind myself I'm doing all this for you.

ACKNOWLEDGEMENTS

The successful completion of this thesis was made possible with the support of many people.

Sincere appreciation is expressed to Dr. J. Amend and the Department of Anatomy & Physiology for the opportunity of doing graduate study in the new facilities of the AVC. I would like to thank my supervisor Dr. D.E. Sims for the opportunity and financial support. Guidance and patient answering of many questions was provided by Drs. J. Burka and F. Markham, my Supervisory Committee. Dr. Burka also provided financial support which was very much appreciated. Many thanks to Dr. A. Donald for his generous help with the statistical aspects of this study. I would especially like to thank Dr. W.P. Ireland who, although not a member of my committee, took me under his wing and provided excellent advice and moral support during the latter phase of this work.

I would like to give special mention to Dianne Friesen (alias Super EM Technician), a wonderful teacher and friend who was always there to help and provide one-on-one tutorials in electron microscope techniques and delicious home cooked food. I would like to thank Sandy Gamble for her technical assistance during the summer of '88. Her incredible sense of humour made the many days in the lab enjoyable. I am greatly indebted to my friend and fellow graduate student, Bryan Grimmelt, for his expert guidance and assistance in spectrophotometry. His help with the computer is also greatly appreciated. I would also like to thank Heather Briand, Rosemary Hood and Barry Connell for their technical support, advice and patience. I would like to take this opportunity to give my sincere thanks to Virginia Kopachevsky and Jennifer Taylor (Interlibrary Loan), Shelley Ebbett (Photography) and Floyd Trainor (Graphics) for their excellent assistance on numerous phases of this work. I would like to thank my friends Carla Smith, Kim Whitman, and Janice Gillis for always being there. Special thanks to Sharon Gormley for typing this thesis.

Finally, I would like to thank my parents for the patience and support they have shown throughout my university education, without them I would not have achieved my goals.

This research project was funded in part by the Natural Science and Engineering Research Council of Canada (NSERC), the National Research Council (NRC) and the Department of Anatomy & Physiology.

TABLE OF CONTENTS

	<i>Page</i>
TITLE	i
CONDITIONS OF USE	ii
PERMISSION TO USE THESIS	iii
CERTIFICATION OF THESIS WORK	iv
ABSTRACT	v
DEDICATION PAGE	vii
ACKNOWLEDGEMENTS	viii
TABLE OF CONTENTS	ix
LIST OF TABLES	xi
LIST OF FIGURES	xii
NOTATION	xv
1. AN INTRODUCTION TO ACUTE INFLAMMATION	1
1.1 Historical Highlights	1
1.2 Mediators Involved in the Vascular Phenomena of Inflammation	2
1.3 The Venule Wall in Inflammation	4
1.3.1 Response of the venule to inflammatory mediators	4
1.3.2 Evidence for endothelial cell contractility	10
1.3.3 Possible role for the pericyte in the modulation of vascular leakage	11
1.3.4 Application of vascular labelling in studies of microvascular permeability	14
1.4 Objectives of This Study	15
2. MONASTRAL BLUE AS A VASCULAR LABEL IN RATS	17
2.1 Introduction	17
2.2 Materials and Methods	19
2.2.1 Experimental animals and anesthetization procedure	19

	Page
2.2.2 Removal time from circulation using skin model	19
2.2.2.1 Light microscopy	21
2.2.2.2 Confirmation of increased vascular permeability	21
2.2.3 Monastral blue concentration in serum	22
2.2.3.1 Spectrophotometry and elimination kinetic	22
2.2.4 Arterial blood pressure monitoring	23
2.2.5 Statistical Analysis	23
2.3 Results	25
2.3.1 Removal time of monastral blue	25
2.3.2 Elimination kinetics of monastral blue	30
2.3.3 Effect of monastral blue on blood pressure	30
2.4 Discussion	34
 3. AN ELECTRON MICROSCOPICAL STUDY OF THE PERICYTE - ENDOTHELIAL CELL RELATIONSHIP IN TRACHEAL, DERMAL AND SKELETAL MUSCLE VENULES	 40
3.1 Introduction	40
3.2 Materials and Methods	42
3.2.1 Vascular perfusion procedure	42
3.2.2 Electron microscopy	44
3.2.3 Stereology	45
3.2.4 Statistical analysis	48
3.3 Results	48
3.3.1 Pericyte coverage of the venule wall in three anatomical locations	49
3.3.2 Comparison of the venule wall thickness in three tissues	54
3.3.3 Pericyte relationship to endothelial cell gaps and junctions	54
3.3.3.1 Chi-square analysis of the pericyte-endothelial cell gap and junction relationship	57
3.4 Discussion	60
3.4.1 Morphology of the venule wall	62
3.4.2 Pericyte - endothelial cell relationship	66
 4. GENERAL SUMMARY AND DISCUSSION.....	 67
REFERENCES	76

LIST OF TABLES

	PAGE
Table.I. Mediators of inflammation and their effects on the microvasculature.	5
Table.II. Mean pericyte coverages and thicknesses of the venule wall in different vascular beds. .	50

LIST OF FIGURES

	PAGE
Fig.1. Standard curve for Monastral Blue in rat serum at 604 nm.	24
Fig.2. Rat abdominal skin showing the six sites of intradermal injection of 30 ul of 10^{-4} M histamine (*). The leaky venules labeled at the -2, 0, 5 and 7 minute post-Monastral Blue infusion sites. No labeling was evident at the 10 and 15 minute sites. x 3.	26
Fig.3. Rat abdominal skin showing the six sites of intradermal injection of 30 ul of 10^{-4} M histamine. All sites (*) showed Evans blue-labeled albumin leakage into the interstitium.	27
Fig.4. Liver sample from a rat given an intravenous infusion of Monastral Blue. Monastral Blue (→) is evident within phagosomes of the Kupffer cells. Hematoxylin and Eosin stain. x 1000.	28
Fig.5. Spleen sample from a rat given an intravenous infusion of Monastral Blue. Monastral Blue (→) is seen within phagosomes of the splenic macrophages in the red pulp. Hematoxylin and Eosin stain. x 1000.	29
Fig.6. Rat serum collected at (L-R) 0 (control), 1, 3, 5, 7 10, 15, 20, and 30 minutes after an intravenous infusion of Monastral Blue. ..	31
Fig.7. Concentration of Monastral Blue in rat serum over time. The concentration of Monastral Blue in serum was determined spectrophotometrically and the log of the concentration plotted as a function of time. The plot was linear indicating first order elimination. Data was best fitted by a one compartment model. Half-life was calculated to be 3.54 ± 1.9 minutes.	32
Fig.8. Effect of Monastral Blue infusion in rats on arterial blood pressure. An intravenous infusion of Monastral Blue consistently caused a significant (*, $p < .0001$) decrease in blood pressure.	33

	PAGE
Fig.9. Whole mount of rat cremaster muscle showing Monastral Blue labeled venules (→). x 50.	35
Fig.10. Epon thick section of cremaster muscle showing Monastral Blue labeled venule. The Monastral Blue appears as sky blue masses (↑) within the vessel wall. Toluidine Blue stain.	36
Fig.11. Electron micrograph of cremaster muscle showing the electron dense rod shaped particles of Monastral Blue (↑) between the endothelium (E) and a pericyte process (P). x 40,000.	37
Fig.12. Low magnification transmission electron micrograph (TEM) of a venule wall in trachea 5 minutes after administration of histamine. Electron dense accumulations of Monastral Blue are evident in the vessel wall (↑) under the pericyte (P) and it's processes (p). A polymorphonuclear leukocyte (pmn) is seen between the endothelium (E) and pericyte process. A degranulated platelet is also apparent (dp). x 8,300.	51
Fig.13. Low magnification TEM of two generations of venules in cremaster muscle 5 minutes after the administration of histamine. Electron dense accumulations of Monastral Blue are apparent within the vessel wall (↑) usually under pericytes (P). Endothelial cell gaps are indicated by astericks (*). A pericyte bridge is seen restricting the extravasation of a platelet and an erythrocyte (▼). The vessel lumen contains platelets (Pl), erythrocytes (Er) and a polymorpho-nuclear leukocyte (pmn). x 3,900.	52
Fig.14. Higher magnification TEM of pericyte-endothelial cell relationship in a dermal venule, showing pericyte processes (p) covering endothelial cell junctions (*). Note contact between pericyte and endothelial cell (↓). Monastral Blue is present beneath the pericyte process (↑). The basement membrane of the pericyte (↓) is continuous with that of the endothelium. x 15,000.	53

	PAGE
Fig.15. High magnification TEM of a dermis venule showing a contact (►) between a pericyte (P) and an endothelial cell (E). An interpericyte contact is also evident (▼). Extravasated erythrocyte (Er) profiles are also seen under pericyte bridges. Numerous layers of basal lamina (↓) are present. x 30,000.	55
Fig.16. Pericyte processes (p) are shown maintaining the continuity of an otherwise disrupted venule wall in cremaster muscle. Monastral Blue (↑) is evident under the pericyte processes. Three endothelial gaps are shown (*), two of them with extravasating erythrocytes (Er). Note space (s) between endothelium (E) and pericyte (P). x 4,000.	56
Fig.17. Dermis venule showing pericyte coverage of Monastral Blue accumulations (↑), an endothelial cell gap (*) and a diapedesing polymorphonuclear leukocyte (pmn). An adipocyte (Ad) appears in the lower right. Collagen fibers are seen in the interstitium (cf). x 5,000.	58
Fig.18. Region of extensive gap formation in cremaster venule showing discontinuous endothelium (E), platelets (Pl) and extravasating erythrocytes (Er). Monastral Blue deposits are retained within the venule wall by both pericyte processes (p) and basement membrane (↓). Nuclear region of a pericyte appears at upper right. x 8,000.	59

NOTATION

C5a	complement protein generated by 5-convertase
C3a	complement protein generated by 3-convertase
PMN	polymorphonuclear leukocyte
HPTE	hydroperoxyeicosatetraenoic acid
HETE	hydroxyeicosatetraenoic acid
AA	arachidonic acid
PG	prostaglandin
TX	thromboxane
NANC	non-adrenergic, non-cholinergic
μm	micrometer or micron
GMP	guanine monophosphate
nm	nanometer
MB	Monastral Blue
BW	body weight
N	number of samples
PE	polyethylene
μl	microlitre
M	molarity
pCO_2	partial pressure carbon dioxide
pO_2	partial pressure oxygen
K^+	potassium
H	histamine
BNF	buffered neutral formalin
RCF	relative centrifugal force
SD	standard deviation
i.v.	intravenous
mmHg	millimeters mercury
wt	weight
$^{\circ}\text{C}$	degrees celsius
G	gauge
mOsm	milliosmolar
\AA	angstrom
TEM	transmission electron microscopy
SEM	scanning electron microscopy
Sv	surface per unit volume
I_l	intersections per length of line on grid
S_o	surface area of pericyte order
S_e	surface area of endothelium
I_o	intersections between grid and pericyte order
I_e	intersections between grid and endothelium
T	thickness
P_b	number of points hitting vessel wall
I_b	number of intersections with vessel wall
d	distance between intersects on grid
ANOVA	analysis of variance
GLM	general linear model
SAS	statistics analysis system
F	F-test statistic
df	degrees of freedom
P	P value or significance value
H&E	Hematoxylin and Eosin

1. AN INTRODUCTION TO ACUTE INFLAMMATION

1.1 Historic Perspective

Inflammation is the response of vascularized tissues to irritation or injury. Inflammation is a protective mechanism because it provides a way for defensive factors, like immunoglobulins, complement and phagocytic cells, to gain direct access from the blood stream to sites of microbial invasion or tissue damage.

Inflammation literally means "a burning". The word itself can be traced back to the origin of medicine. A word that can be translated as inflammation appears several times in the Smith Papyrus, a scroll written in Egypt around 1650 B.C. (1) This scroll was derived from an original perhaps 1000 years older. The symbol for inflammation, the flaming brazier, conveys the idea "hot thing" and was used in connection with wounds. With reference to wounds the Greeks at the time of Hippocrates used the term phlegmone, the "fiery thing". (1)

The Roman encyclopedist Cornelius Celsus provided a clinical definition of inflammation which has not since been substantially improved. (2) His description of the major signs of inflammation was RUBOR ET TUMOR CUM CALORE ET DOLORE "redness and swelling with heat and pain". A fifth sign FUNCTIO LAESA, "disturbed function", was added around 1882 by

Rudolph Virchow in his book Cellular Pathology. These are now termed the cardinal signs of inflammation.

By the middle 19th century Julius Conheim, a student of Virchow, had described the vascular changes caused by inflammation.(3) In 1883, Elie Metchnikoff noted the activities of the "wandering mesodermal cells" and demonstrated that phagocytosis was a defense mechanism against irritants.(3)

1.2 **Mediators Involved in the Vascular Phenomena of Acute Inflammation**

Reactive changes that occur in the first few hours after sublethal tissue injury involve:

1. Changes in vascular calibre and flow
2. Increased permeability resulting in the formation of inflammatory exudates and local edema.
3. Escape of leukocytes from the blood into extravascular tissues.

These phenomena are varied and complex. Each injury or stimulus may result in a different mix of these processes, a different time course and a different outcome.

Both direct and chemically mediated injury to the microcirculation take place in an acute inflammatory response. Direct leakage results from damage to the vessel (e.g., a burn) by the injurious agent itself. Chemically mediated

leakage (e.g., vasoactive mediators), although postulated almost a century ago by Cohnheim(3), was not recognized until recently. This form of vascular alteration is an active phenomena that occurs not only in the area of injury but also peripheral to that area. In simplest terms, an inflammatory mediator can be described as a chemical substance acting on blood vessels and/or cells to contribute to an inflammatory response. The term "autacoid" which means "self remedy" has also been applied to chemical mediators. It refers to a variety of substances of intense pharmacological activity that are normally present in the body, but cannot be conveniently classed as neurohumors or hormones.

Chemical messengers may be exogenous mediators (produced outside of the cell) or endogenous mediators (produced within the cell). Plasma contains three major mediator-producing systems (kinins, coagulation factors, and complement cascade) which interact in a complex, defined manner to generate phlogistic compounds. Other mediators are cell-derived, including those preformed and stored in granules (e.g., histamine) or those newly synthesized by the cells (e.g., eicosanoids, platelet activating factor, interleukin -1).

Many peptide mediators are generated as a consequence of multiple enzymatic steps, which involve sequential activation of molecules by limited proteolysis (complement and coagulation systems). Small fragments derived from such steps may also exhibit biological activity (e.g., C5a, C3a).

Lipid mediators are generally synthesized "de novo" within cells upon activation. Arachidonic acid, derived from membrane phospholipids, is a precursor to a wide variety of molecules, collectively termed eicosanoids. Examples of mediators involved in vascular alterations are given in Table 1. The table provides an overview of different types, their status in tissues, and the source and action of some central compounds. Several mediators produce the same effect and the relative importance of one mediator versus another is often difficult to assess. Mediators with similar actions may have different levels of importance depending on the tissue involved and the stimulus for injury (46). As a further complication, some mediators can be responsible for more than one of the vascular or cellular changes in inflammation (see Table 1). A frequent action of these mediators is an increase in vascular permeability ("Tumor").

1.3 The Venule Wall in Inflammation

1.3.1 Response of the venule to inflammatory mediators

The classic studies of Majno et al (5,6,7) demonstrated that inflammatory mediators (histamine and similar agents) produce endothelial cell separation and a selective increase in macromolecular permeability. This response is confined to post-capillary venules. There is very strong evidence that

TABLE 1

MEDIATOR	STATUS IN TISSUE	MAJOR SOURCE	MAIN BIOLOGIC ACTIVITY	SELECTED REFERENCES
<u>AMINES</u>				
Histamine	Preformed	Mast cells, basophils	Increases vascular permeability, induces hypotension	(4,5,6,7,8,9)
5-Hydroxy-tryptamine	Preformed	Platelets, mast cells	Increases vascular permeability, induces hypotension	(10,4,11,12)
<u>LIPIDS</u>				
HPETE* and HETE**	Newly synthesized from AA via the lipoxygenase pathway	Arachidonic Acid	Potent chemotactic substances for PMN Leukocytes, vasoconstriction	(13)
5-HETE	Newly synthesized from AA via the lipoxygenase pathway	Arachidonic Acid	Stimulates histamine release from mast cells	(12)

* hydroperoxyeicosatetraenoic acid

** hydroxyeicosatetraenoic acid

MEDIATOR	STATUS IN TISSUE	MAJOR SOURCE	MAIN BIOLOGIC ACTIVITY	SELECTED REFERENCES
Leukotriene C ₄ , Leukotriene D ₄ , Leukotriene E ₄	Newly synthesized from AA via the lipoxygenase pathway	Arachidonic Acid	Smooth muscle contraction and increased vascular permeability, stimulates PG synthesis	(14,15,16)
Leukotriene B ₄	Newly synthesized from AA via the lipoxygenase pathway	Arachidonic Acid	Chemokinesis and chemotaxis of leukocytes, increased vascular permeability, induces TXA ₂ synthesis	(14,15,17)
Prostaglandin E's Prostaglandin I ₂	Newly synthesized from AA via cyclooxygenase pathway	Arachidonic Acid	Vasodilator enhances the vasopermeability induced by other mediators by increasing blood flow, augments PMN leukocyte emigration	(18,19,20,21,22, 23,24)
Prostaglandins F ₂ ^α Thromboxane A ₂	Newly synthesized from AA via the cyclooxygenase pathways	Arachidonic Acid	Vasoconstriction, immunomodulators	(18,19,20,21,22, 23,24)
Platelet-activating factor	Newly synthesized phospholipid	Membrane Lipids	Induces platelet secretion, neutrophil secretion, increased vascular permeability, hypotensive	(25,26,27)
Interleukin - I		Macrophages, human epidermal cells	Chemoattractant for neutrophils	(28,29)

<u>MEDIATOR</u>	<u>STATUS IN TISSUE</u>	<u>MAJOR SOURCE</u>	<u>MAIN BIOLOGIC ACTIVITY</u>	<u>SELECTED REFERENCES</u>
<u>PEPTIDES</u>				
Kinins	Preformed as kininogen	Plasma globulins (kininogens)	Vasodilation, increased vascular permeability, pain	(30,31,32,33,34)
Fibrinogen breakdown products	Released from fibrinogen by action of thrombin or released during proteolysis of fibrin by plasmin	Blood clot	Increased vascular permeability chemotactic for neutrophils	(35)
C ₃ _a and C ₅ _a	Preformed as part of antigen	Complement	Mast cell degranulation, smooth muscle contraction, neutrophil chemotaxis (C ₅ _a), enhances vascular permeability induced by other mediators	(36,37,29)
Vasoactive Intestinal Peptide	Preformed peptide	NANC nerves in lung and gastrointestinal tract	Vasodilator	(38,39)
Substance P	Preformed peptide	NANC nerves in the airways	Potent promoter of vascular permeability	(40,41,42)
Calcitonin gene related peptide	Preformed peptide	Afferent nerves in the airways	Potent arteriolar vasodilator and potentiator of edema	(43,44,42)
Neuropeptide Y	Preformed peptide	Nerves innervating blood vessels in human lung	Potent constrictor of vascular smooth muscle	(45,42)

this type of leakage is due to active contraction of endothelial cells, which in turn causes transient and reversible openings to form in junctions between adjacent cells (7). This type of leakage has been shown to play a role in the early stages of fluid and protein loss after many kinds of injury.

The findings of Majno and his co-workers have been repeated and extended by others, utilizing intravital light microscopy, fluorescent macromolecular probes with well defined molecular weights, and direct measurements of mediator stimulated macromolecular efflux (47,48,49,50,51). These studies demonstrated that mediator stimulated increases in macromolecular efflux are dependent on the formation of discrete macromolecular leakage sites in venules.

Mediator-induced leakage is confined exclusively to postcapillary venules; cell junctions in other vascular segments are not affected by these agents. However, venules of similar size and structure in different tissues vary in their response to permeability factors. In any particular tissue the response is the same whether permeability factors are applied topically or injected intravascularly (52,53).

Current knowledge of tissue specificity to mediators may be summarized as follows:

1. Venules adjacent to many surfaces of the body and in loose connective tissues are sensitive to histamine and similar agents. Such tissues include skin and

subcutaneous tissues, skeletal muscle, serous membranes like pleura and peritoneum, lip, conjunctiva, and the mucosa of the trachea and large bronchi.

2. Venules in solid organs including testis, kidney, salivary glands and the central nervous system, and vessels in the mucosa of the small intestine fail to respond to mediators (53).
3. Pulmonary alveolar capillaries and venules are also insensitive to permeability factors (54,55). This is probably due to a lack of receptors for the mediators. The reason for this variable response is not completely understood. Clearly it may be most misleading to draw generalized conclusions as to the mechanism of any particular type of injury from its effects in only one tissue. Vessels of apparently identical structure may, in other situations, respond in quite different ways to the same type of injury.

Palade et al. (56) suggested that the special features of the venular endothelium are probably more important for the pathophysiology of the vascular endothelium (i.e., inflammatory reactions) than for its physiological permeability properties. Venules are also a site of predilection for hemorrhage, thrombosis and diapedesis, as well as allergic and thermal injury.

The endothelial cells of post capillary venules of the skin can be stimulated repeatedly by mediators without loss of their regulatory capacity (50,57). By active formation

and closure of gaps in the post capillary venules, these venular endothelial cells may thus regulate the macromolecular efflux from the microcirculation. Leukocyte adhesion and migration to the interstitium also occurs in post capillary venules. There is also the possibility that gap formation together with other factors might participate in the regulation of cellular escape from venules (21).

1.3.2 Evidence for endothelial cell contractility

It is now generally well accepted that active contraction of the endothelial cell is the most plausible mechanism underlying gap-formation under the influence of histamine-type mediators (58). Evidence in support of this view has come from numerous studies on modulation of the permeability of microvascular endothelium to macromolecules (59,57,16) and small solutes (60). In addition to ultrastructural evidence, the phenomenon has been observed in vivo (61,58) as well as in cultured endothelial cells exposed to histamine or thrombin (62, 63). The presence of microfilaments within endothelial cells is strong circumstantial evidence for endothelial contractility (64,65). The composition of these microfilaments has been characterized by immunostaining with antibodies to various contractile proteins including actin, myosin, α -actinin or tropomyosin (65,66). These filaments are arranged in a way that could produce a sliding filament

mechanism of contraction and cell shortening (66). It has also been demonstrated that mediator receptors are located along the cell junctions in the venule. Localization of histamine receptors has recently been performed using histamines coupled to ferritin (67). The conjugates preferentially bind to H_2 receptors and the endothelial cytoplasm next to the binding sites was found to be particularly rich in filaments.

It has recently been shown that endothelial cells possess a cisternal system similar to smooth muscle cells that could provide the means for a release of cytosolic calcium in response to receptor activation (68). Studies using calcium-chelating agents such as EDTA (69) or endothelial cell stabilizers (70) have counteracted the contractile effects of the inflammatory mediators.

Anti-inflammatory agents including vasopressin, β -adrenergic agonists, antihistamine, glucocorticoids and methylxanthines reverse the contraction of endothelial cells seen in response to inflammatory mediators (57).

1.3.3 Possible role for the pericyte in the modulation of vascular leakage

The venule wall is composed of endothelial cells, pericytes and their associated intercellular materials. Endothelial cells of post capillary venules appear to harbour receptors for mediators of permeability, supporting the idea

that endothelial cells are the site of pro and anti-inflammatory actions of various agents. However, most investigations of permeability alterations in venules have dealt only with the endothelial cell, leaving out possible contributions of other mural elements.

Histamine-induced gaps are large enough (0.5-1 μm in diameter) for proteins, platelets, erythrocytes and even leukocytes to escape from the venule (4,5). Formed elements are not, however, routinely extravasated during histamine reactions. Components of the venular wall, other than endothelial cells, including endothelial cell basal laminae, pericytes and the pericytic basal lamina appear to be candidates for mediating extravasation of formed elements and macromolecules.

Pericapillary (adventitial) cells, originally described by Rouget in 1873 and termed pericytes by Zimmerman in 1923 (review by 71) are distinctive cells of mesodermal origin that envelop microvessels with their elongate bodies and multiple, branching foot processes (72). Pericytes contain α -smooth muscle actin (73) myosin (74), tropomyosin (75) and an enzyme related to smooth muscle function, GMP dependent protein kinase (76). Using immunofluorescent and immunoelectron microscopic labelling both desmin and vimentin, components of intermediate filaments found in contractile cells, have also been identified (77). It has also recently been shown that cultured bovine retinal pericytes exert a tonic form of

contractile stress upon their collagen lattice substrate (78).

Pericytes are enveloped in a basal lamina which is continuous with the basal lamina of the blood vessel, thus distinguishing it from other vessel associated cells (72). There is in vitro evidence that pericytes contribute to the production of this basal laminar substance (79). Pericytes are intimately associated with endothelial cells. An intercellular distance of less than 20 nm is often noted between them, and a variety of junctions between pericytes and endothelial cells have been reported (71).

Ultrastructural characteristics of venules and pericytes and possible physiologic roles of pericytes have been recently reviewed (80,71). Pericytes are most numerous on postcapillary venules, so numerous in fact that some investigators (81) refer to these venules as pericytic venules.

Pericyte processes have been reported to occur in close proximity to endothelial cell junctions in bovine lung capillaries (82). In human choriocapillaris capillaries in the eye (83) and rat dermal capillaries (84) pericytes have been shown to be strategically located to provide minimal interference with nutrient and gas exchange. The positions and roles of pericytes on venules, however, are as yet largely unexplored. The anatomical location of pericytes places them in a unique position to modulate leakage from venules.

Pericytes and their basal lamina appear to block extravasation of macromolecules and blood-borne elements when leakage has been induced by histamine or serotonin (4,5), bradykinin (85) or thermal injury (86,87). In venules, leaked proteins and tracer particles are frequently trapped under pericytes or their basal lamina (86,87,88). Most recently it has been demonstrated that pericytes prevent the extravasation of plasma platelets, erythrocytes, and occasionally leukocytes from the cytoplasmic gaps in the walls of delicate developing endothelial walls during capillary growth (89).

Control of macromolecular movement across the venule wall and restriction of inflammatory cell migration to the interstitium are thus two more possible functions of the pericyte. Pericytes should be included as components of the venule wall which participate in histamine-mediated inflammatory events.

1.3.4 Application of vascular labelling in studies of microvascular permeability.

The technique of vascular labelling is an experimental procedure whereby those vessels of the microcirculation that have become abnormally permeable (without being totally disrupted) can be identified by light as well as by electron microscopy. By virtue of their size (50-500 nm) certain colloidal suspensions injected intravenously will leave the blood through endothelial gaps, but will not be able to

traverse basal laminae of endothelial cells and pericytes. They become trapped within the vessel wall, thereby labelling sites of extravasation for subsequent study (88). The original labels, colloidal carbon (5) and mercuric sulphide (90) are no longer commercially available. Monastral blue (MB) is a copper phthalocyanine pigment which, when prepared as a colloidal suspension, has many of the desired properties of a vascular label (88). MB's intense color, sharp contrast and electron density make it a potentially valuable tool in electron microscopic studies of inflammation.

1.4 Objectives of this study

Although increased vascular leakage in response to inflammatory mediators is confined exclusively to post-capillary venules, very few studies have investigated the ultrastructural characteristics of the venule wall in a state of increased vascular permeability. The venule wall is composed of endothelial cells, pericytes and their basal laminae, yet no one has attempted to quantify the pericyte-endothelial cell relationship in venules. All studies looking at the pericyte coverage of vessels have been conducted on capillaries (91,92,82,93,94). Investigations into pericyte orientation and possible roles for the pericyte on venules are lacking.

The work presented in this thesis was designed to 1) examine the pericyte-endothelial relationship in venules of three different vascular beds (trachea, dermis and cremaster muscle); 2) establish whether the percentage of pericyte coverage was the same in these different anatomical locations; 3) compare separate venule wall thicknesses; and 4) determine whether pericyte coverage of endothelial gaps and junctions is random or not. Appropriate results would therefore suggest a role for the pericyte in modulation of vascular permeability.

This work required the use of the vascular label Monastral Blue. However discrepancies in the literature about its effectiveness necessitated an additional technical study to 1) determine how long MB remained available in the vascular system to label leaky venules; 2) measure MB concentration in serum over time using spectrophotometry; and 3) characterize possible cardiovascular effects due to MB infusion.

2.

MONASTRAL BLUE AS A VASCULAR LABEL IN RATS

2.1

Introduction

Increased vascular permeability with formation of a richly proteinaceous edema is one of the cardinal signs ("tumor") of acute inflammation. Vascular labelling with tracer substances is an established technique that permits the identification of leaky microvessels. The procedure requires intravascular infusion of colloidal particles which then become trapped in the wall of the vessel if its endothelial barrier has been interrupted, but basement membrane has remained intact.

The labelling technique has been applied to studies of microvascular inflammation (95,96,97) and injury (55,98). The classical studies of Majno et al. (4,5,6,7) demonstrated that inflammatory mediators (histamine and similar agents) produce endothelial cell separation and a selective increase in macromolecular permeability. This response is confined to post capillary venules. There is strong evidence that this type of leakage is due to active contraction of endothelial cells which creates transient and reversible openings in junctions between adjacent cells (7). A pigment that is trapped in vessel walls at sites of increased permeability "labels" these sites for subsequent light and electron microscopy (88). Because the original vascular tracers,

colloidal carbon and mercuric sulfide, are no longer commercially available, new substitutes have been sought. Monastral blue (MB) is a copper pthalocyanine pigment which, when prepared as a colloidal suspension, has many of the desired properties of a vascular label (88).

The original description of MB as a vascular label stated it would remain in the vascular system of the rat for an hour before being removed by the mononuclear phagocytic system (88). Takagi et al. (99) speculated that MB was effectively removed from the rat circulation within 15 minutes. A study of neurogenic inflammation using MB as the label recently reported the half-life of MB in rats to be only 3.4 ± 0.1 minutes (100).

Joris et al. (88), in the original evaluation of MB, observed that, following intravenous injection of MB, rat lung would return to a normal pink color within minutes. There was no sign of respiratory distress and hepatocytes were not damaged. They concluded that MB was a suitable stable, nontoxic vascular tracer when injected in a dosage of 0.1 ml/100g. However, Albertine and Staub (101) found that in anesthetized sheep MB caused physiological side effects (i.e., systemic hypotension, pulmonary hypertension and bronchoconstriction) when infused and concluded that the vascular tracer is not biologically inert in sheep. Species differences may therefore be pertinent when considering the usefulness of MB.

Such discrepancies in the literature about the effectiveness of MB prompted a study to re-evaluate MB as a vascular label in the rat. The goals of this present study were to (1) determine how long MB remained available in the vascular system to label microvessels, (2) measure the MB concentration in serum as a function of time, and (3) characterize cardiovascular effects of MB.

2.2 Materials and Methods

2.2.1 Experimental animals and anesthetization procedure

Male Sprague Dawley rats (200-250 gm, Charles River Canada Inc., St. Constant, Que., N=28) were used in accordance with accepted principles (102). Rats were anesthetized with halothane (initially in a bell jar) using a nonbreathing anesthetic circuit (Co-axial Bain Circuit, Hoechst) at a rate of 2.5 volume percent with a fresh gas flow of oxygen at 0.7 litres/min. Rectal temperature was monitored with a thermal probe and maintained at 35 ± 2 °C with a warming pad. A pinch test was used to assure surgical anesthesia.

2.2.2 Removal time from circulation using rat skin model

PE-50 polyethylene catheters (Intramedic, Becton Dickinson and Company, Parsippany, New Jersey) were placed in

the right femoral vein for drug infusion and left femoral artery for pressure monitoring. The catheters contained heparinized saline. On the midventral surface of the abdomen 6 points were selected for injection sites. Monastral blue (3% suspension in nonionic surfactant and biocide; Sigma Chemical Co., St. Louis, MO) was administered as a bolus over about one minute at the recommended dose of 0.1 ml/100g of body weight (88). Localized areas of leakage from post capillary venules were then created by injecting 30 μ l of 10^{-4} M histamine dihydrochloride (Sigma) into the abdominal dermis at -2, 0, 5, 7, 10 and 15 minutes with respect to the intravenous infusion of MB. An additional site was injected with lactated Ringer's injection vsp (Travenol Canada Inc., Mississauga, Ont.) at 5 min post MB, as well, to show the injection procedure itself was not creating leaky vessels. Ten minutes after the last injection of histamine a blood sample was drawn from the right femoral artery and the rat was euthanized with an over dose of halothane followed by an intracardiac injection of 2 ml of a saturated solution of potassium chloride in distilled water. Blood samples were immediately analyzed with a Nova Biomedical Stat Profile 4 Blood Gas Analyzer for pH, pCO_2 , PO_2 and K^+ .

Four rats were pretreated with the H_1 -antihistamine, mepyramine maleate B.P. (Poulenc, Montreal), as controls to demonstrate leaky venules were due to the direct action of histamine. The H_1 blocker was given by intravenous infusion

of 2 mg/kg of body weight in lactated Ringer's solution 10 minutes before the injection protocol (103,104).

2.2.2.1 Light microscopy

The abdominal skin was removed, gently stretched and pinned on cardboard. Injection sites were examined for labeled venules using a binocular dissecting microscope. After initial observations the skin was fixed in 10% buffered neutral formalin (BNF) for 48 hours, then cleared with two changes of glycerol over two weeks and re-examined.

Samples of the liver and spleen from each rat were removed at the end of each experiment. They were immersion fixed in 10% BNF for 48 hours, then dehydrated in graded alcohols and embedded in paraffin. Hematoxylin and eosin (H&E) stained tissue sections were examined with a light microscope for MB deposits.

2.2.2.2 Confirmation of increased permeability

Five additional rats were treated similarly to those described above except that they received an intravenous infusion of Evan's Blue (Sigma) of 0.2g/kg BW of body weight as a 5% solution lactated Ringer's solution 10 minutes before the injection schedule began. Evan's Blue acts as a marker for plasma extravasation by binding to plasma albumin. This

amount of Evan's Blue presumably did not exceed the binding capacity of circulating plasma albumin in the rat, based on studies of the binding capacity of plasma albumin of other species (105,106).

2.2.3 Monastral Blue concentration in serum over time.

Four rats were used to analyze the concentration of MB in serum over time, to assess the rate of MB removal by the mononuclear phagocytic system. PE-50 catheters were placed in the right femoral vein for MB and Ringer's solution infusion and the left femoral artery for blood withdrawal. Blood samples (0.5 ml aliquots) were drawn on the following schedule with respect to the infusion of MB: 0 (control), 1, 3, 5, 7, 10, 15, 20 and 30 minutes. For each unit of blood removed an equal volume of lactated Ringer's solution was concurrently replaced to maintain blood volume. The dilution factor caused by adding lactated Ringer's solution to the vascular system was taken into consideration when calculating results.

2.2.3.1 Spectrophotometry and elimination kinetics

Blood samples were centrifuged at 1500 RCF (Beckman T-J6 Counter Top Centrifuge) for 10 minutes; serum was collected and diluted five fold with distilled water. Levels of MB were measured by diode array spectrophotometry at 604 nm (Hewlett

Packard model 8452A, HP ChemStation analysis software). Standards were prepared by adding MB to serum from untreated rats, Fig.1. The zero time (pre-MB control) serum sample was used as a blank for each rat.

2.2.4 Arterial blood pressure monitoring

The left femoral artery catheter in all the rats except the four used for serum collection was connected to a Gould P23 series pressure transducer. Blood pressure was monitored continuously during the experiments and recorded on a linear chart recorder (Gould, Cleveland, OH). A Blood Pressure Systems Calibrator (Bio-Tek Instruments Inc., Winooski, VT) was used to calibrate the transducer to a range of 0-200 mmHg.

2.2.5 Statistical analysis

Student T-tests were performed with the MINITAB^R statistics package. A probability value of 0.05 was used to determine statistical significance. Data are expressed as mean \pm SD.

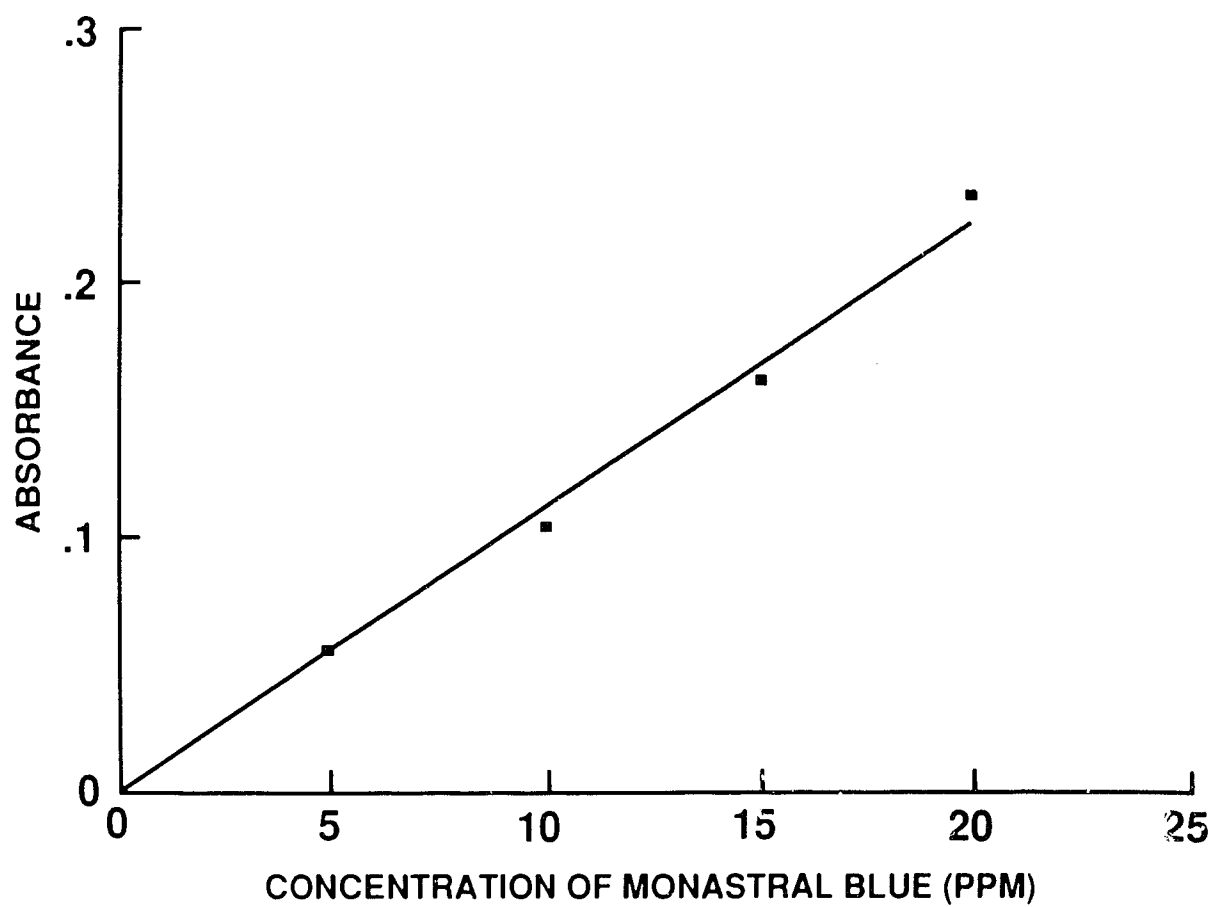


Fig.1. Standard curve for Monastral Blue in rat serum at 604 nm.

2.3 Results

2.3.1 Removal Time of Monastral Blue

Monastral Blue labelling of venules was apparent in the -2, 0, 5 and 7 minute injection sites in all the rats tested. Labeling was not seen in the 10 and 15 minute sites in any of the rats (Fig.2). Analysis of skins immediately after removal and after subsequent fixing and clearing showed essentially the same results, MB being somewhat easier to detect in cleared skins.

Control rats pretreated with the H₁-antihistamine, mepyramine maleate, and sites given Ringer's solution injections in place of histamine at no time showed labeling or edema. Some mepyramine blocked the response, the leakage is probably due to H₁ receptor activation in the venules of the rats.

Evan's Blue leakage into the interstitium occurred in all six injection sites of all four animals tested (Fig.3). Blood gases and electrolytes always remained within normal ranges (102) ruling out complications due to alterations in acid/base balance or electrolytes.

Examination of the H&E stained tissue samples revealed abundant MB particles within the Kupffer cells of the liver and the splenic macrophages (Fig.4&5), the constituents of the mononuclear phagocytic system responsible for removing 90% of i.v. injected particle suspensions (107).

National Library
of Canada

Canadian Theses Service

Bibliothèque nationale
du Canada

Service des thèses canadiennes

NOTICE

AVIS

THE QUALITY OF THIS MICROFICHE
IS HEAVILY DEPENDENT UPON THE
QUALITY OF THE THESIS SUBMITTED
FOR MICROFILMING.

UNFORTUNATELY THE COLOURED
ILLUSTRATIONS OF THIS THESIS
CAN ONLY YIELD DIFFERENT TONES
OF GREY.

LA QUALITE DE CETTE MICROFICHE
DEPEND GRANDEMENT DE LA QUALITE DE LA
THESE SOUMISE AU MICROFILMAGE.

MALHEUREUSEMENT, LES DIFFERENTES
ILLUSTRATIONS EN COULEURS DE CETTE
THESE NE PEUVENT DONNER QUE DES
TEINTES DE GRIS.

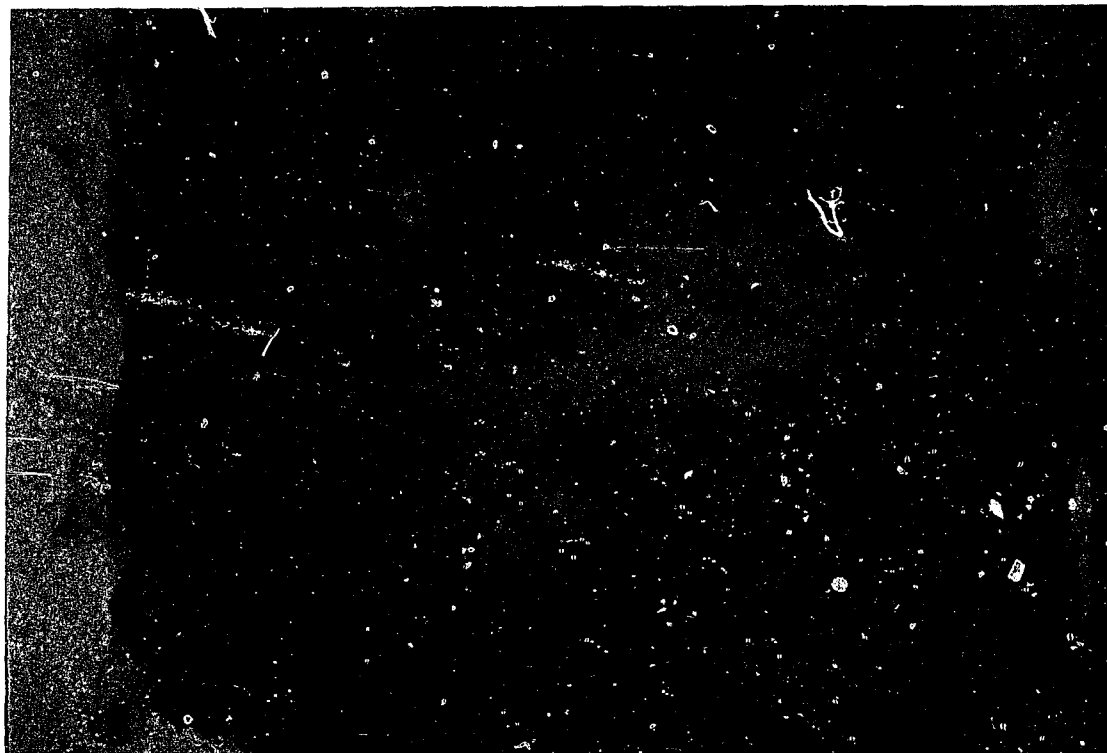


Fig.2. Rat abdominal skin showing the six sites of intradermal injection of 30 μ l of 10^{-4} M histamine (*). The leaky venules labeled at the -2, 0, 5 and 7 minute post-Monastral Blue infusion sites. No labeling was evident at the 10 and 15 minute sites. x 3.

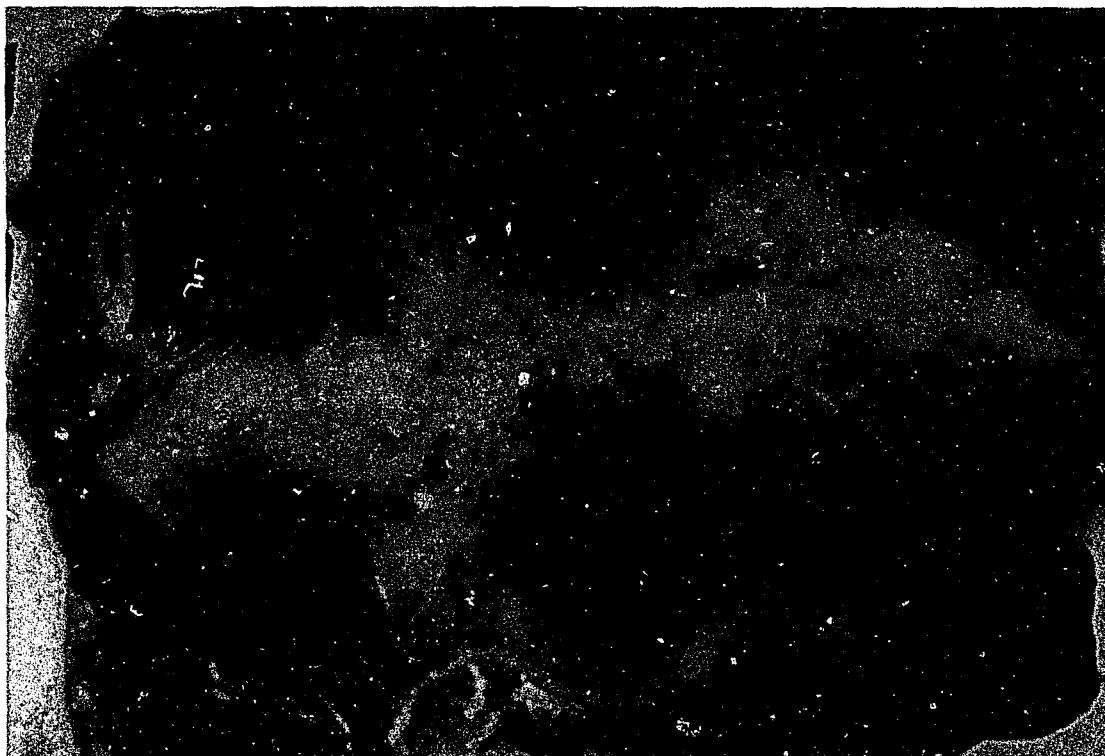


Fig.3. Rat abdominal skin showing the six sites of intradermal injection of 30 ul of 10^{-4} histamine. All sites (*) showed Evans blue-labeled albumin leakage into the interstitium.

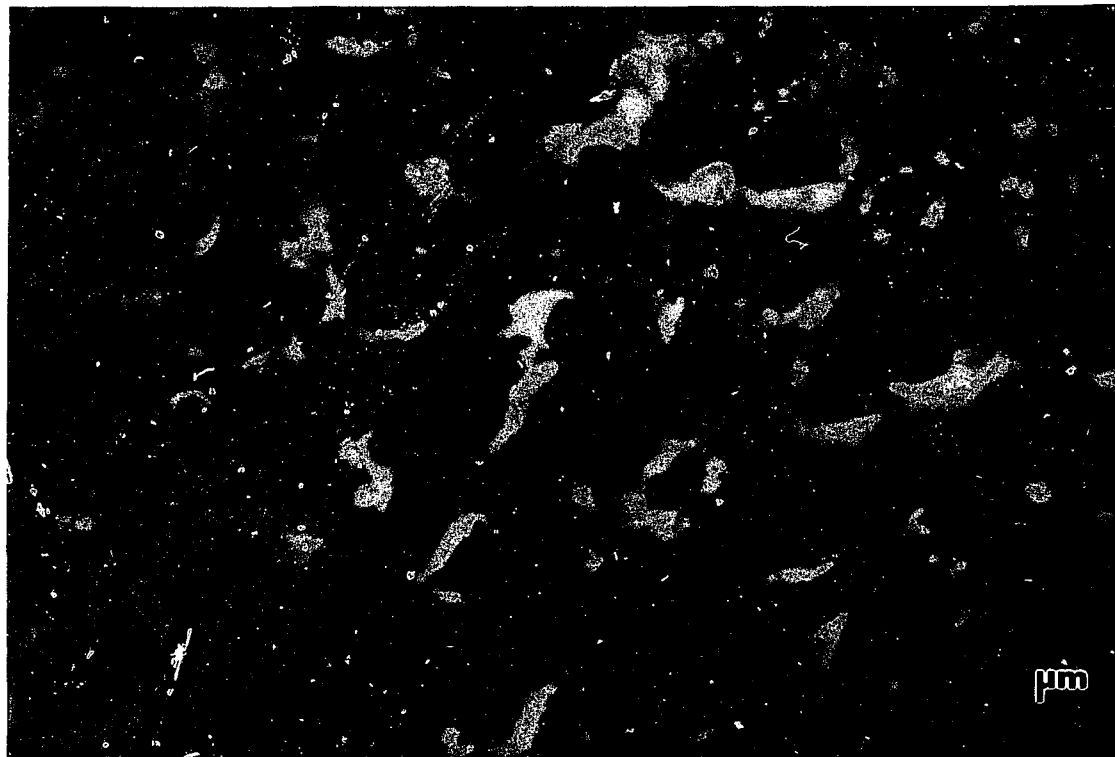


Fig.4. Liver sample from a rat given an intravenous infusion of Monastral Blue. Monastral Blue (→) is evident within phagosomes of the Kupffer cells. Hematoxylin and Eosin stain. x 1000.

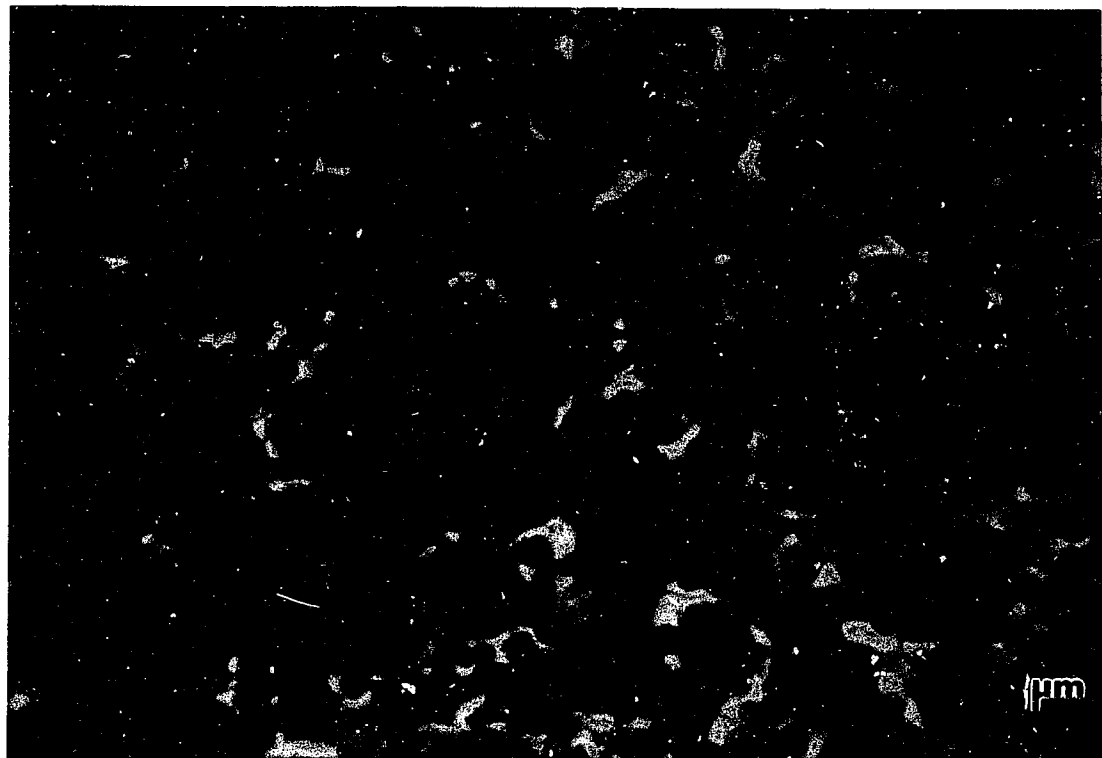


Fig.5. Spleen sample from a rat given an intravenous infusion of Monastral Blue. Monastral Blue (→) is seen within phagosomes of the splenic macrophages in the red pulp. Hematoxylin and Eosin stain. x 1000.

2.3.2 Elimination Kinetics of Monastral Blue

Spectrophotometric analysis of rat serum taken after the infusion of MB revealed that elimination of MB from the vascular system was rapid and showed first order kinetics (Figs. 6&7). The estimate of the half life was 5.54 ± 1.9 minutes and that of the apparent mean volume of distribution was 0.9 l/Kg. Data was best fitted by a one compartment model.

2.3.3 Effect of Monastral Blue on Blood Pressure

Infusion of MB caused a significant drop in arterial blood pressure (Fig. 8). The mean arterial pressure dropped from a pre-infusion value of 82 ± 14 to 58 ± 18 mmHg ($N=19$, $p<.0001$). This represents a $30 \pm 13\%$ (mean \pm SD, $p<.0001$) decrease, reaching the lowest value by 1.08 ± 0.3 minutes post infusion. The pressure did recover to pre-MB values by 10 minutes in all of the experiments. Evan's Blue infusion had no effect on blood pressure. Pretreatment with the H_1 -antihistamine, mepyramine maleate, did not block the hypotensive response.

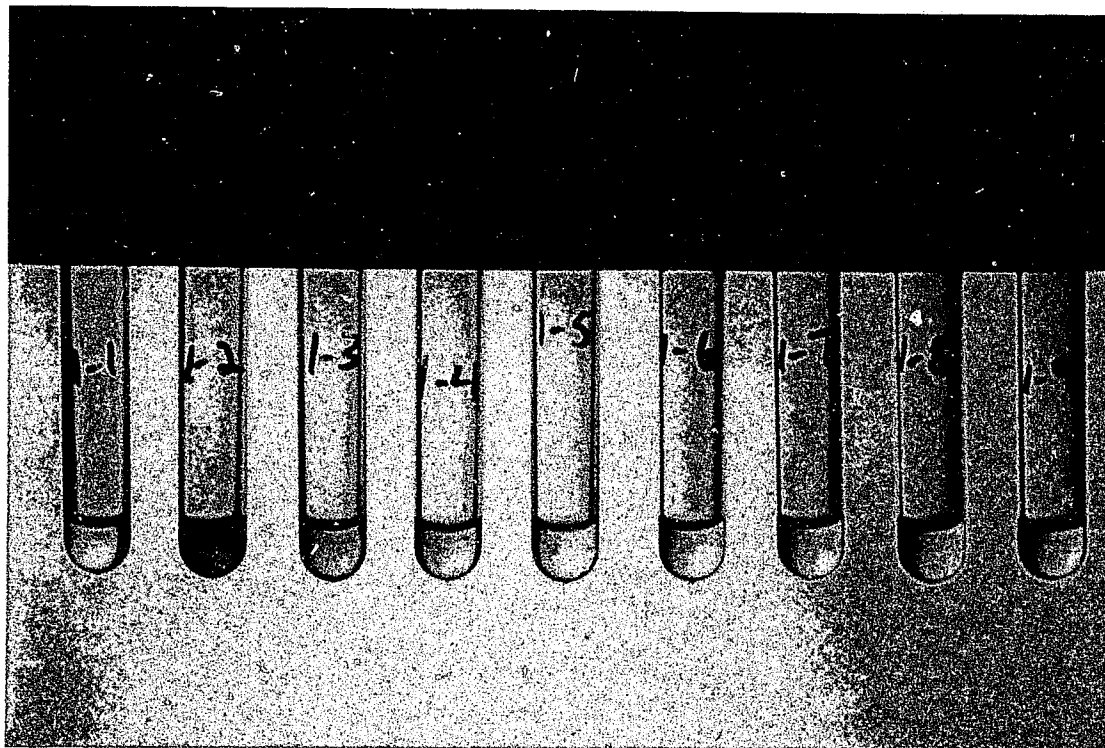


Fig.6. Rat serum collected at (L-R) 0 (control), 1, 3, 5, 7, 10, 15, 20, and 30 minutes after an intravenous infusion of Monastral Blue.

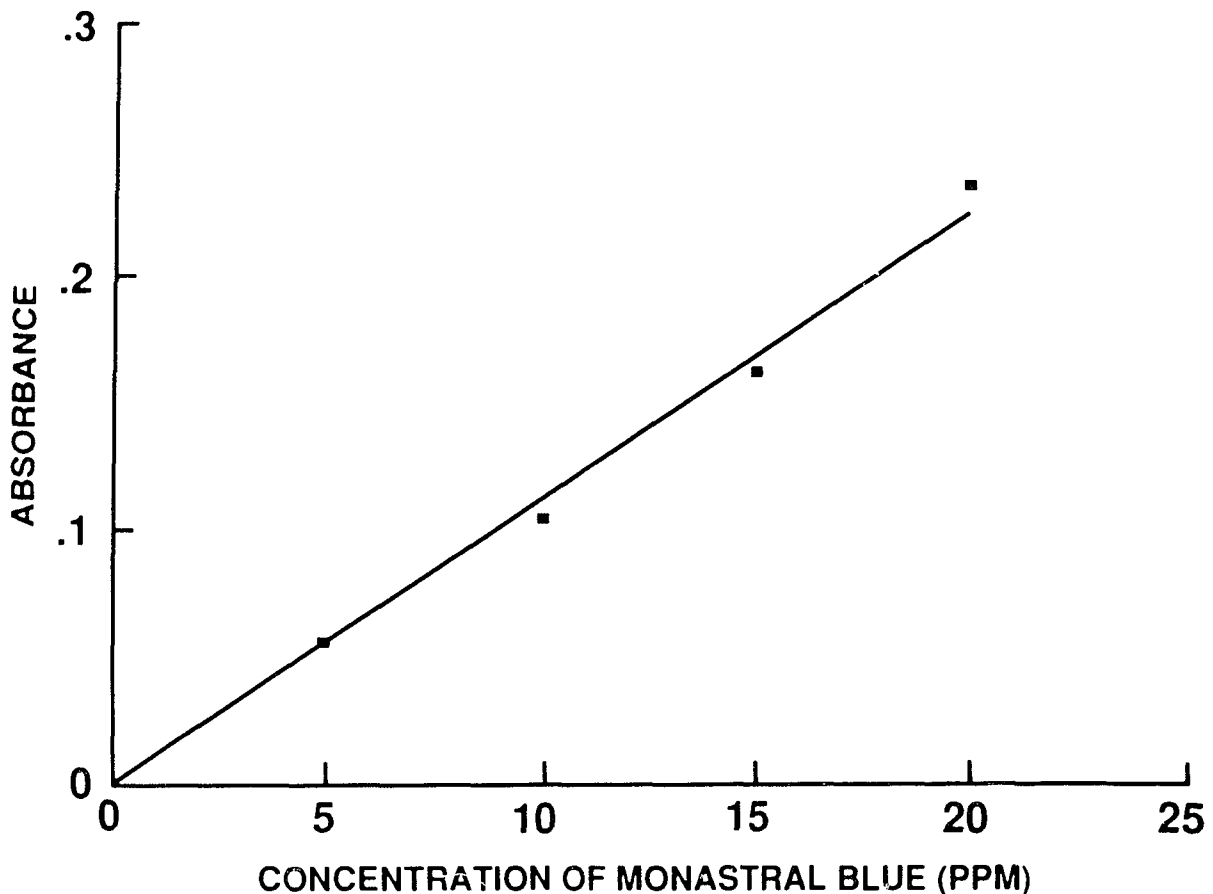


Fig.7. Concentration of Monastral Blue in rat serum over time. The concentration of Monastral Blue in serum ($\mu\text{g}/\text{ml}$) was determined spectrophotometrically and the log of the concentration plotted as a function of time. The plot was linear indicating first order elimination. Data was best fitted by a one compartment model. Half-life was calculated to be 3.54 ± 1.9 minutes and the mean volume of distribution to be 0.9 l/Kg . ($N=4$)

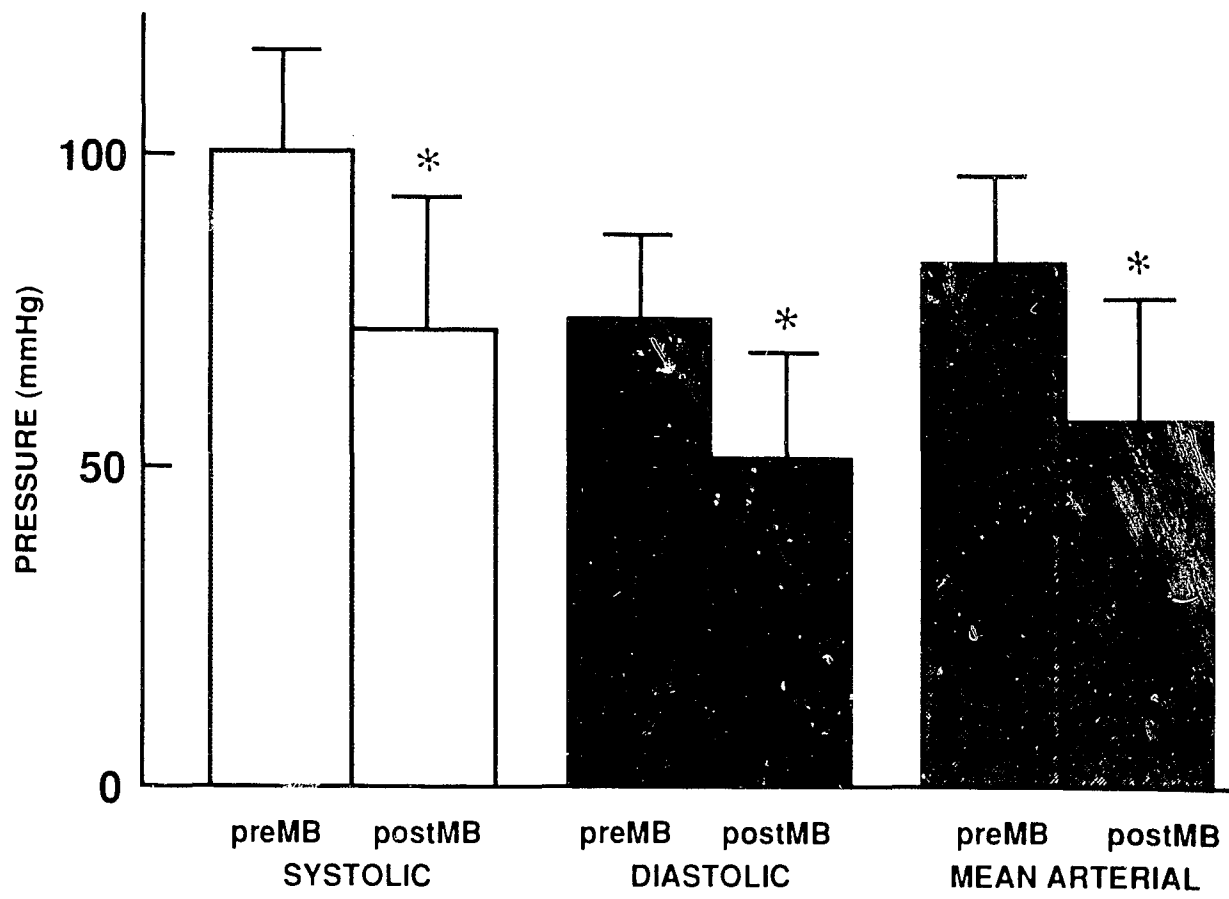


Fig.8. Effect of Monastral Blue infusion in rats on arterial blood pressure. An intravenous infusion of Monastral Blue consistently caused a significant (*, $p < .0001$) decrease in blood pressure.

2.4 Discussion

The extravasation of MB occurs through gaps between endothelial cells of venules. Three dimensional reconstructions of endothelial gaps caused by histamine show that the gaps caused by histamine always occur at endothelial intercellular junctions, often exceed 0.5 μm in width, are very irregular in shape, and do not involve a complete separation of the junctions (47). Mediator induced contraction of endothelial cells is thought to participate in the formation of such gaps (7,61)

By virtue of its size (50-300 nm) MB can leave the blood through endothelial gaps but cannot traverse the basal laminae of the endothelial cells and pericytes. It is trapped within vessel walls, thereby labelling the sites of extravasation (88). Monastral blue can be detected in venule walls with the naked eye (Fig.9), light microscopy (Fig.10) and electron microscopy (Fig.11) (this study;88). MB has also been described as stable and nontoxic when given in the order of 0.1 - 0.2 ml/100 gm body wt., fulfilling the criteria of a suitable vascular label (88). There are, however, conflicting reports concerning just how long MB remains within the vascular system available to label abnormally permeable blood vessels (88,99,100). In this study it was observed that MB injected intravenously, in the standard dose of 0.1 ml per 100 gm body weight, caused the rat's extremities to become blue.

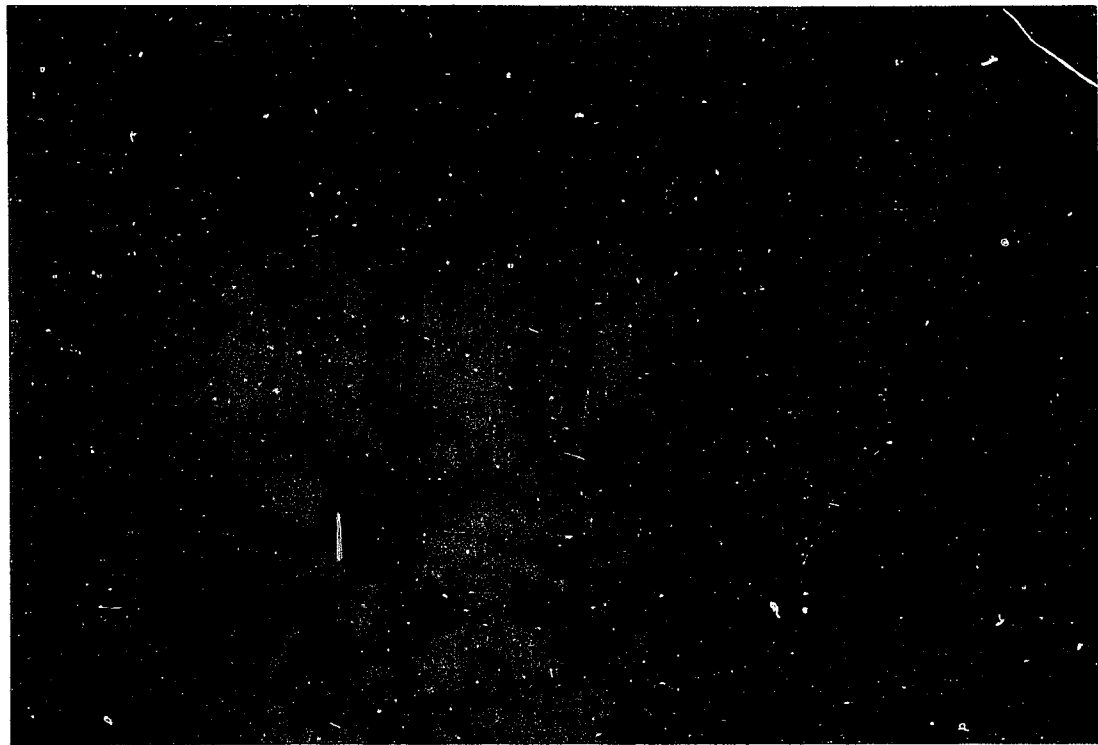


Fig.9. Whole mount of rat cremaster muscle showing
Monastral Blue labeled venules (→). x 50.



Fig.10. Epon thick section of cremaster muscle showing Monastral Blue labeled venule. The Monastral Blue appears as sky blue masses (↓) within the vessel wall. Toluidine Blue stain. x 400



Fig.11. Electron micrograph of cremaster muscle showing the electron dense rod shaped particles of Monastral Blue (↑) between the endothelium (E) and a pericyte process (P). $\times 40,000$.

After about 5 minutes, the natural color appeared restored. Sites of histamine injections given at 10 and 15 minutes after the infusion of MB to induce abnormal permeability in venules do not become labelled even though Evan's Blue-albumin complexes in the interstitium confirm plasma leakage has occurred. It was concluded from these results that enough MB is removed from the bloodstream by the mononuclear phagocytic system within 10 minutes that its effectiveness as a label is limited to about 7 minutes (half life 3.54 ± 1.9 min). This time frame, which is much shorter than the original description of the vascular labels (88), was supported by the spectrophotometrically-determined serum concentrations. The one compartment model of kinetics indicates a very rapid distribution phase that presumably occurred before the first sample was taken. The apparent mean volume of distribution backs up the one compartment model because 0.9 l/Kg compares to reported blood volumes for rats (106).

In this study, MB infusion into rats caused a significant decrease in the arterial blood pressure. Pressure recovered in about 10 minutes, coinciding with the clearance time of MB from serum. These results are similar to the findings of Albertine and Staub (101), who were the first group to suggest that MB is not biologically inert as described by Joris (88) and can cause physiological side effects in sheep.

Histamine release in response to vascular tracers has been a concern of investigators who use them. Histamine

liberation did not appear to be an important factor in this study because an H₁ antagonist did not block the pressure drop observed. This physiological effect of MB should be taken into consideration in studies where cardiovascular parameters are measured.

Monastral blue still has specific usefulness in permeability studies in preference to tracers like Evan's blue. Tracers do not reveal the precise locations of the abnormally permeable blood vessels or the morphological basis of the permeability change, because the extravasated dye quickly diffuses away from the sites of leakage and is not visible by electron microscopy. In contrast, intravascular labels, such as MB, actually become part of the vascular structure being studied.

In conclusion, monastral blue as a vascular label meets the needs of light and electron microscopic studies but has some restrictions: it will cause a drop in blood pressure and it is effectively removed from the vascular system within 7 - 10 minutes by the mononuclear phagocytic system. Thus experiments utilizing MB should be designed with these limitations in mind.

3. AN ELECTRON MICROSCOPIC STUDY OF THE PERICYTE-ENDOTHELIAL CELL RELATIONSHIP IN TRACHEAL, DERMAL AND SKELETAL MUSCLE VENULES.

3.1 Introduction

The role and significance of pericytes within the microvasculature remains unresolved, although a variety of functions have been postulated for them. These include mechanical support of the capillary wall (72), active phagocytosis of deposits within the vascular wall during and after the inflammatory reactions (108,109,4,5), biosynthesis of basement membrane and collagen (79), and regulation of capillary proliferation (110,111). Recently Orlidge and D'Amore (112) demonstrated that pericytes suppress or modulate endothelial growth in vitro. Pericytes may also have a contractile function and be responsible for local blood flow regulation (92). Pericytes are likely precursors of smooth muscle cells (74). Recently, Rhodin (89) provided evidence that fibroblasts are transformed into pericytes, and pericytes into smooth muscle cells during capillary growth and differentiation in the rat mesentery.

Pericytes have also been observed to serve as reinforcements for the very delicate and leaky walls of capillary sprouts (89). Plasma and extravasated formed elements of the blood accumulate under pericytes, temporarily transforming them into umbrella shaped cells. Pericyte

modulation of vascular leakage may be retained in the fully developed microvascular bed. This function should be particularly demonstrable in the post capillary venules where the inflammatory response is very well established (4,5,95,85,71). A gradient of permeability which begins in the arterioles reaches a peak in the post capillary venule and then decreases gradually along the veins (113). Diapedesis of white blood cells occurs here in response to a variety of stimuli (114). As well, inflammatory mediators, such as histamine, act on this segment to produce endothelial cell contraction and gap formation resulting in increased vascular permeability (4,5).

Pericytes are most numerous on post capillary venules (81). However, specific roles of pericytes during inflammation have not been extensively investigated.

In the present study electron microscopy and morphometric techniques were employed to quantitatively assess the relationship of pericytes to endothelial cells during histamine-induced vascular permeability. The pericyte coverage of venules from three different microvascular beds was investigated to see if venules in varying anatomical regions exhibit the same population of pericytes. A comparison of vessel wall thickness was also made. Skeletal muscle, dermis and trachea venules are all sensitive to histamine and similar vasoactive agents. Skeletal muscle and dermis have been the models used in most investigations of

mediator-induced vascular permeability because of their accessibility and reactivity (4,56,49). Plasma leakage from the tracheobronchial microvasculature is now being linked with many facets of the pathophysiology of airway diseases such as asthma (115,116). For these reasons venules from skeletal muscle, dermis and trachea were selected for this study. The relative position of pericytes to endothelial cell junctions and gaps was also studied to determine if pericytes are strategically located over them. Such information would contribute to a better understanding of the cellular response during inflammation.

3.2 Materials and Methods

3.2.1 Vascular perfusion procedure

Male Sprague Dawley rats (200-250 gm, Charles River Canada Inc., St. Constant, Que., N=5) were used in accordance with accepted principles (102). Rats were anesthetized with halothane (initially in a bell jar) using a non-breathing anaesthetic circuit (Co-axial Bain circuit, Hoechst) at a rate of 2.5 volume percent with a fresh oxygen flow at 0.7 litres/min. Rectal temperature was monitored with a thermal probe and maintained at 35 ± 2 °C with a warming pad. Animals were placed in the supine position. A pinch test was used to assure surgical anesthesia.

An incision was made along the midventral region of the neck and the sternohyoid muscles carefully separated to expose the trachea. The jugular veins on both sides were then exposed (to be cut during fixation) using the collarbone as landmark. Exposed tissue was covered with saline soaked gauze to prevent drying. A midventral incision was made in the abdomen and the right kidney located. The dorsal aorta below the renal vein was carefully separated from the vena cava and a ligature thread passed under it to facilitate locating it at time of perfusion. The body cavity was closed using a hemostat.

PE-50 polyethelene catheters (Intramedic, Becton Dickinson and Company, Parsippany, New Jersey) containing heparinized saline were placed in the right femoral vein for vascular label infusion and the left femoral artery for monitoring pressure. Blood pressure was monitored continuously with a Gould P23 series pressure transducer and recorded on a linear chart recorder (Gould, Cleveland, OH). A Blood Pressure Systems Calibrator (Bio-Tek Instruments Inc., Winooski, VT) was used to calibrate the transducer to a range of 0-200 mmHg. A small incision was made in the scrotal skin and a portion of each cremaster muscle carefully exposed.

Monastral blue (3% suspension in nonionic sulfactant and biocide; Sigma chemical Co., St. Louis, MO) was administered as a bolus over one minute at the recommended dose of 0.1 ml/100 g of body weight (88). Thirty ul of 10^{-4} M histamine

dihydrochloride (Sigma Chemical Co.) was then injected into the lumen of the trachea, intradermally into the abdomen skin and dripped on one of the exposed cremaster muscles to create an increased permeability in the post capillary venules. As controls, the contralateral cremaster muscle and portions of trachea and abdomen dermis remote from the experimental sites were selected for study receiving all identical treatment except for the histamine injection.

Four minutes later a 20 G cannula was inserted into the dorsal aorta for perfusion fixation and the jugular veins cut to allow for rapid efflux of perfusate. Approximately 75 ml of oxygenated heparinized saline (adjusted to 320 mOsm with dextrose) at room temperature were perfused through the animal to clear the circulation of blood. This was followed by a fixative (100 ml/kg) which consisted of oxygenated 2% glutaraldehyde in .05 M sodium cacodylate buffer (pH 7.4, adjusted to 320 mOsm with dextrose) at room temperature. The fixative was administered under a pressure of 100-150 mm Hg. The total time allowed for perfusion was 10 minutes.

3.2.2 Electron Microscopy

Perfusion-fixed specimens were excised immediately, trimmed in 1 mm cubes and immersed in fresh fixative for 1 hour. Tissues were washed in .05 M sodium cacodylate buffer (pH 7.4, adjusted to 320 mOsm with dextrose) and postfixed in

1% osmium tetroxide in .05 M sodium cacodylate buffer. The tissue was washed in distilled water and then dehydrated in a graded series of ethanol, cleared in propylene oxide and filtrated with an epon araldite mixture. After polymerization 0.5 μm sections were cut with glass knives and placed on glass slides, stained with 1% toluidine blue and surveyed for labelled venules. Thin sections (700-900 $^{\circ}\text{A}$) were cut with a diamond knife and placed on 200-mesh copper grids. Grids were contrasted with a saturated solution of uranyl acetate in 50% ethanol and Sato's lead stain (117). Sections were examined using a Hitachi H-7000 transmission electron microscope. Monastral blue labelled venules were photographed. Electron micrographs were processed for analysis.

3.2.3 **Stereology**

The ratio of surface of pericyte to surface of endothelium (percent pericyte coverage) and the thicknesses of the venule wall were investigated. The distribution of pericytes on the venule was also studied to see if pericytes are randomly disposed. Venules were identified by the presence of the vascular label Monastral blue in the vessel wall.

The trace of a surface on a two-dimensional section is a line. The length of this line is proportional to the amount of surface (118). By measuring the length of that line the

surface of tissue can be estimated. Having established that the surface of the endothelium and the surface of the pericyte coverage are lines, the length of these lines can be calculated by randomly placing a grid over the micrographs and counting the intersections of grid line with the surface of interest. The surface area was calculated by the following formula:

$$S_v = 2I_l , \quad (118)$$

where S_v is surface per unit volume and I_l is intersections per length of line.

Pericytes on a venule wall are very numerous and tend to overlap. Therefore a definition of pericyte order was required. The designation of pericyte order was based on the number of pericytes that intervened between the pericyte of interest and the vessel wall. For example, if no pericytes intervened the pericyte was designated first order and if one pericyte intervened it became second order, etc. Intersections between the grid and the following surfaces were counted:

- 1) The abluminal surface of the endothelium
- 2) The adluminal surface of the first order pericytes, second order pericytes and third order pericytes.

Veil cells (fibroblasts) were not included in the measurements.

Since only the ratio of surfaces was of interest, ratios of intersections were calculated between pericytes of

different order and the endothelium. This can be shown to equal the ratios of surface areas, represented by the formula:

$$\frac{S_o}{S_e} = \frac{I_o}{I_e}$$

where S_o is the surface area of pericyte order, S_e is the surface area of the endothelium, I_o is the number of intersections between the grid and the pericyte order and I_e is the number of intersections between the grid and the surface of the endothelium.

By using the same grid that was used for determining surface ratios the thickness of the vessel wall can be determined. One additional count is required, that of grid intersects falling on the vessel wall. Thickness in microns was calculated using the formula:

$$T = \frac{P_b}{I_b} \cdot d \quad (118)$$

where P_b stands for the number of points hitting the wall, I_b for the number of intersections with the wall and d is the distance between intersects (18.8mm divided by the magnification of the electron micrograph).

For purposes of determining whether pericytes are strategically placed over endothelial junctions and gaps, the following counts were made: endothelial cell junctions covered by pericytes, junctions not covered by pericytes, endothelial cell gaps covered by pericytes and gaps not covered by pericytes.

3.2.4 Statistical Analysis

A three way analysis of variance was used to compare percent coverages by pericyte and vessel wall thickness in the three tissues. The factors were tissue, animal and pericyte order for surface ratios, and tissue and animal for thicknesses. Because the number of observations varied between the cells of the ANOVA design, it was necessary to use the GLM (General Linear Model) procedure in the SAS System Statistical package (119). Where the F test indicated there was a significant difference between treatments individual means were compared using Sheffe's test, which is appropriate when the number of observations varies between cells (120).

To determine if the coverage of endothelial junctions or gaps by pericytes was random, the expected (% coverage x total number of junctions or gaps) and observed (number of junctions or gaps covered by pericytes) percentages of covered junctions or gaps were compared using a Chi-square goodness of fit test (121).

3.3 Results

Five minutes after administration of histamine, a variety of ultrastructural changes could be detected in the venule wall of the three tissues studied. Monastral blue accumulation under pericytes and the basal lamina was evident

in trachea (Fig.12), cremaster muscle (Fig.13), and dermis (Fig.14) enabling positive identification of venules. There was an abundance of pericytes and pericyte processes visible in all three tissues as well. Other indications of an acute inflammatory reaction seen in all the tissues included platelet adherence, neutrophil margination, endothelial gap formation and neutrophil diapedesis. Qualitatively, there were more endothelial gaps observed in the cremaster muscle as compared to trachea and dermis.

Control tissues, at no time, showed any indication of vascular labelling or edema. Therefore, absence of change in vascular permeability was assumed.

3.3.1 Pericyte coverage of the venule wall in three anatomical locations

The mean percent coverages by pericytes and their standard deviations are reported in Table II. Analysis of variance revealed that atleast one of the tissues had a significant difference in mean pericyte coverage ($F=5.08$, $df\ 2,84$, $p\leq0.0083$). A Sheffe's test indicated that the significance was due to the difference in coverage between dermis and cremaster muscle venules. There was no significant difference in coverage in second and third order pericytes between the different tissues.

TABLE II Mean pericyte coverages and thicknesses of the venule wall in three tissues. (N=5, Mean \pm SD)

	Trachea	Dermis	Cremaster
% coverage of first order pericytes	82 \pm 12	71 \pm 20*	85 \pm 18*
% coverage of second order pericytes	21 \pm 14	16 \pm 9	24 \pm 2
% coverage of third order pericytes	8 \pm 6	6 ¹	9 \pm 8
Mean thickness of the vessel wall (μ m)	1.68 \pm .92	1.74 \pm .82	1.97 \pm .77

* Dermis and cremaster were significantly different (p=.0083)

¹ Only one sample available

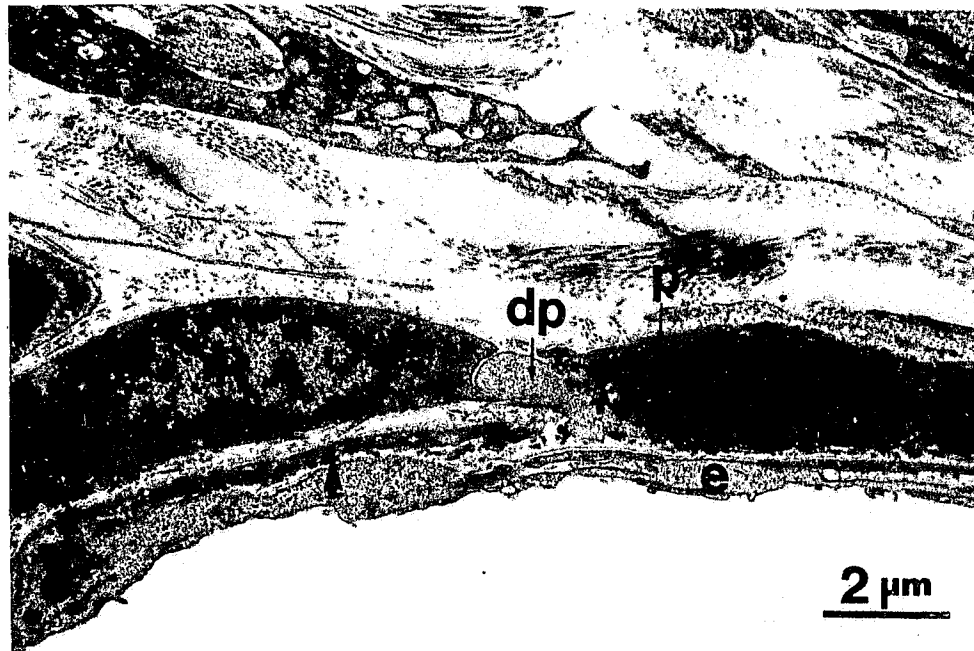


Fig.12. Low magnification transmission electron micrograph (TEM) of a venule wall in trachea 5 minutes after administration of histamine. Electron dense accumulations of Monastral Blue are evident in the vessel wall (↑) under the pericyte (P) and its processes (p). A polymorphonuclear leukocyte (pmn) is seen between the endothelium (E) and pericyte process. A degranulated platelet is also apparent (dp). $\times 8,300$.

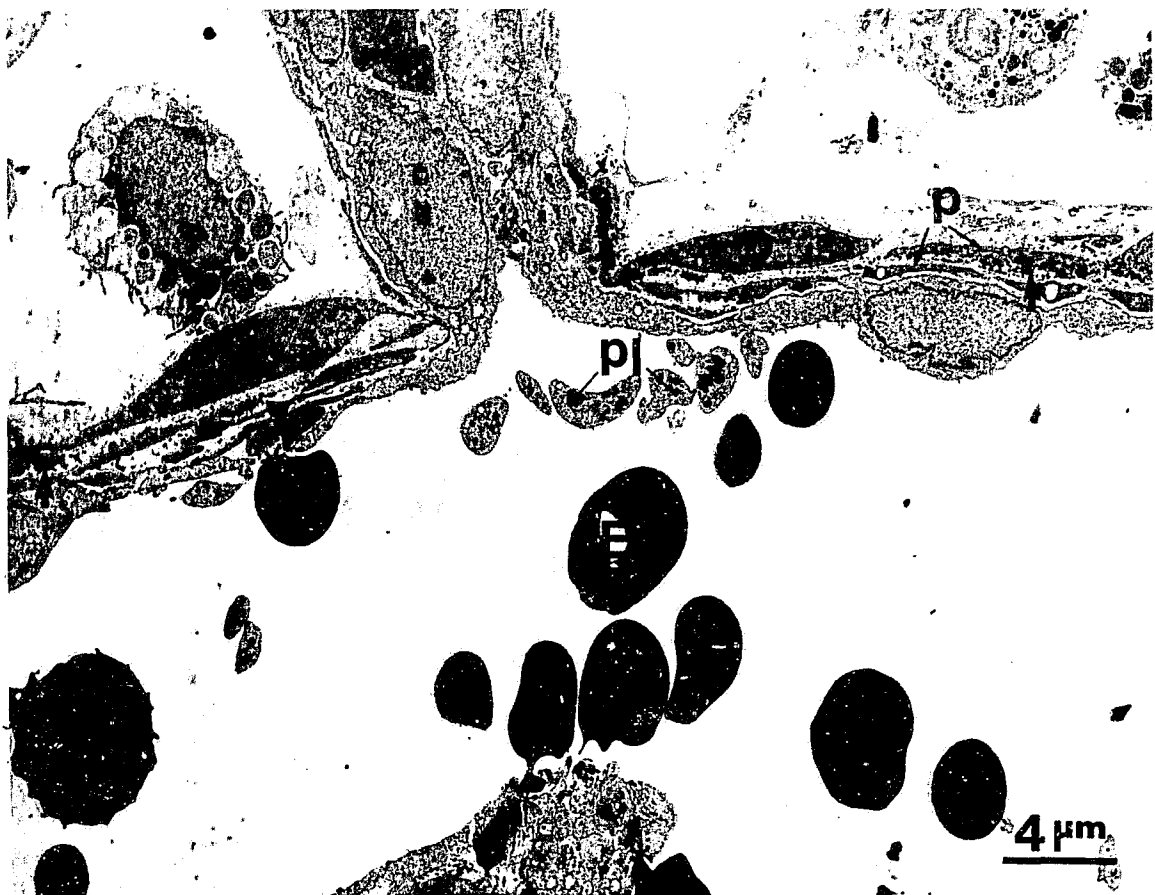


Fig.13. Low magnification TEM of two generations of venules in cremaster muscle 5 minutes after the administration of histamine. Electron dense accumulations of Monastral Blue are apparent within the vessel wall (↑) usually under pericytes (P). Endothelial cell gaps are indicated by astericks (*). A pericyte bridge is seen restricting the extravasation of a platelet and an erythrocyte (▼). The vessel lumen contains platelets (Pl), erythrocytes (Er) and a polymorphonuclear leukocyte (pmn). x 3,900.



Fig.14. Higher magnification TEM of pericyte-endothelial cell relationship in a dermal venule, showing pericyte processes (p) covering endothelial cell junctions (*). Note contact between pericyte and endothelial cell (↓). Monastral Blue is present beneath the pericyte process (↑). The basement membrane of the pericyte (↓) is continuous with that of the endothelium. $\times 15,000$.

3.3.2 Comparison of venule wall thickness

The F value from the analysis of variance showed that at least one of the tissues had a significant difference in mean vessel thickness. However Sheffe's test could not distinguish the difference. This may be because Sheffe's test is a more stringent test than the F test. Mean vessel thicknesses are reported in Table II.

3.3.3 Pericyte relationship to endothelial cells

Pericytes are highly branched and flattened against the connective tissue aspect of the endothelium (72). They do not form a complete cell layer but leave parts of the endothelium separated from the interstitial tissue by only a basement membrane. There is an overlapping of pericytes in some areas giving the impression of several layers of pericytes.

Examination of random sections of the venule wall revealed numerous pericyte processes and endothelial cell junctions (Fig. 13). Typically, the pericyte processes were completely unsheathed by basement membrane which was continuous with that of the endothelium (Fig. 14). There were frequent contacts between the pericytes and the endothelium and pericytes also exhibited contacts with each other (Fig. 15). Most frequently the pericyte process formed a "bridge" over endothelial cell junctions and gaps (Figs. 13, 14&16).

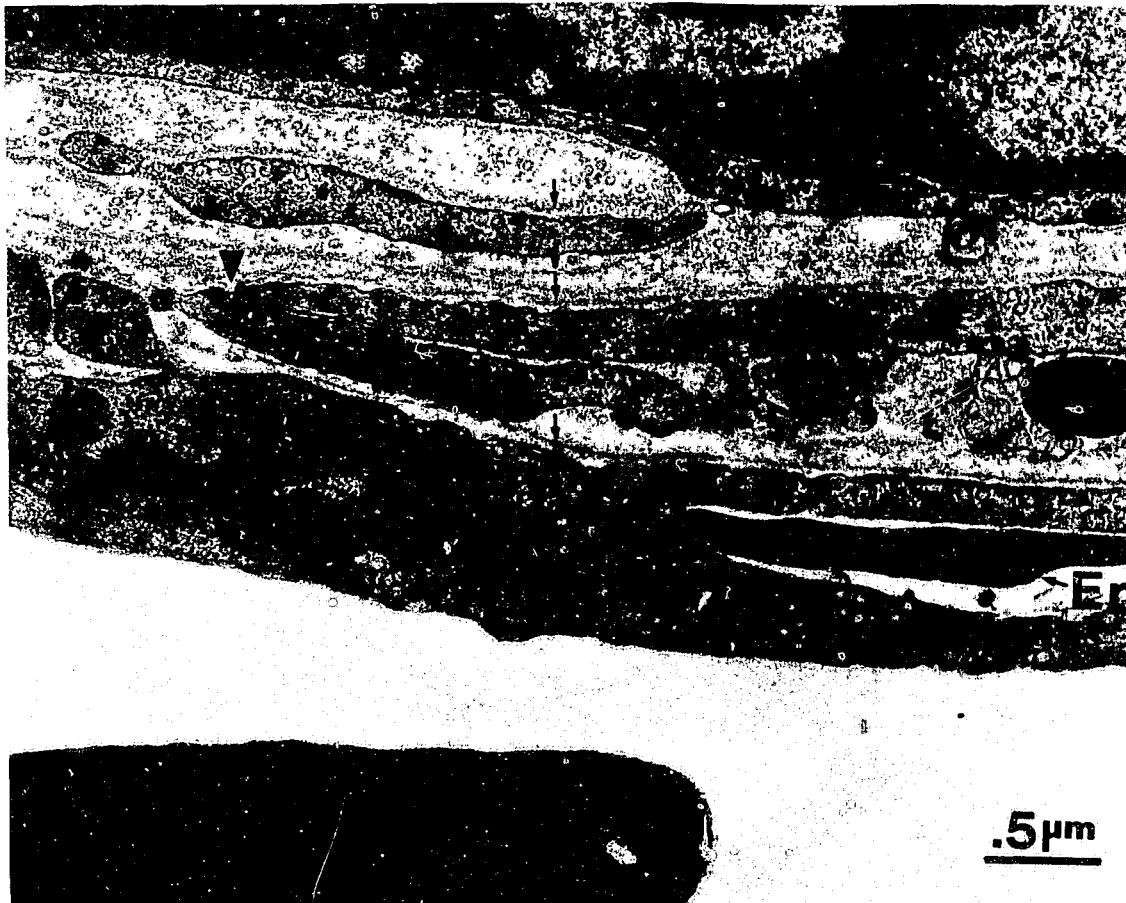


Fig.15. High magnification TEM of a dermis venule showing a contact (►) between a pericyte (P) and an endothelial cell (E). An interpericyte contact is also evident (▼). Extravasated erythrocyte (Er) profiles are also seen under pericyte bridges. Numerous layers of basal lamina (↓) are present. x 30,000.

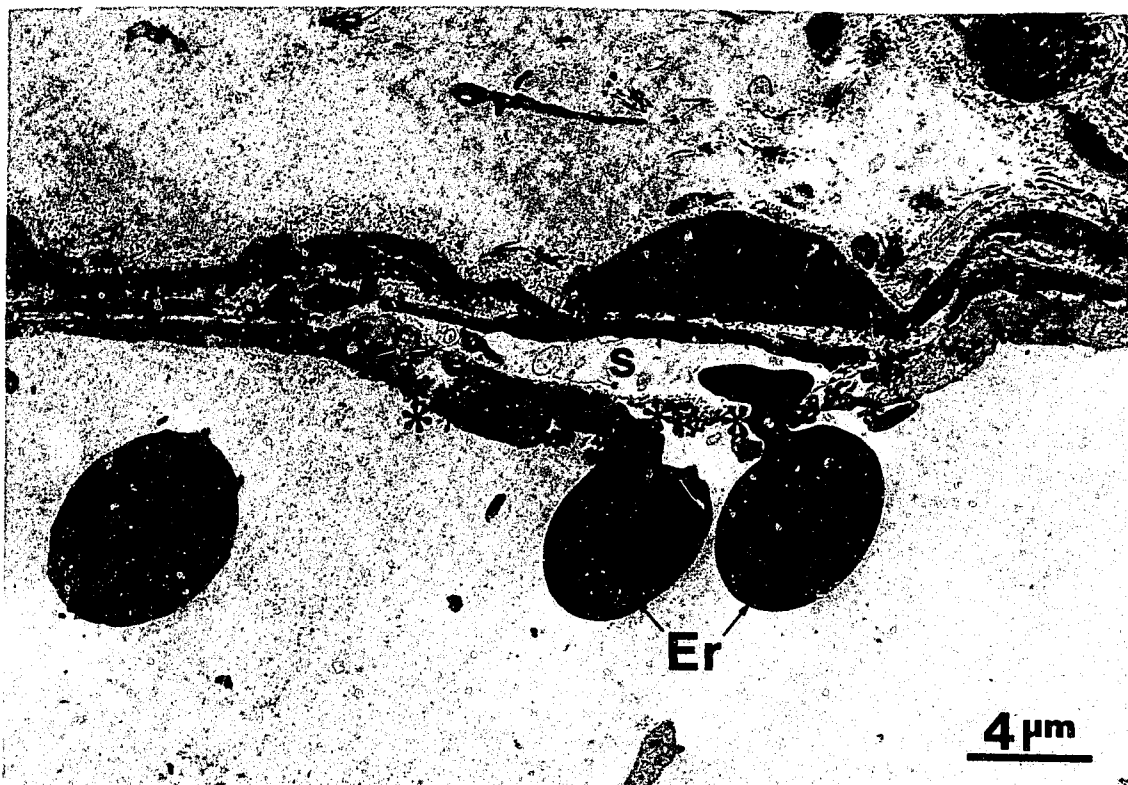


Fig.16. Pericyte processes (p) are shown maintaining the continuity of an otherwise disrupted venule wall in cremaster muscle. Monastral Blue (↑) is evident under the pericyte processes. Three endothelial gaps are shown (*), two of them with extravasating erythrocytes (Er). Note space (s) between endothelium (E) and pericyte (P). $\times 4,000$.

The pericytes were often seen restricting the extravasion of red blood cells, platelets, and accumulating Monastral blue dye along their border and under their basement membrane (Figs. 12,13,16,17&18). Neutrophils were commonly observed in various stages of diapedesis, moving between the endothelium and pericytes (Fig. 6&17).

3.3.3.1 Chi-square analysis of pericyte-endothelial cell gap and junction relationships.

The Chi-square tests comparing the expected and observed numbers of endothelial gaps covered by pericytes were significant for cremaster muscle only. The observed and expected number of covered gaps were not significantly different in the other two tissues. The significance of a chi-square test implies that the pericytes are strategically located over an endothelial gap when it occurs.

The chi-square tests comparing the expected and observed numbers of endothelial cell junctions covered by pericytes were significant in both dermis and cremaster but not in trachea. The significance implies that pericytes are not randomly scattered over a venule but are arranged over junctions.

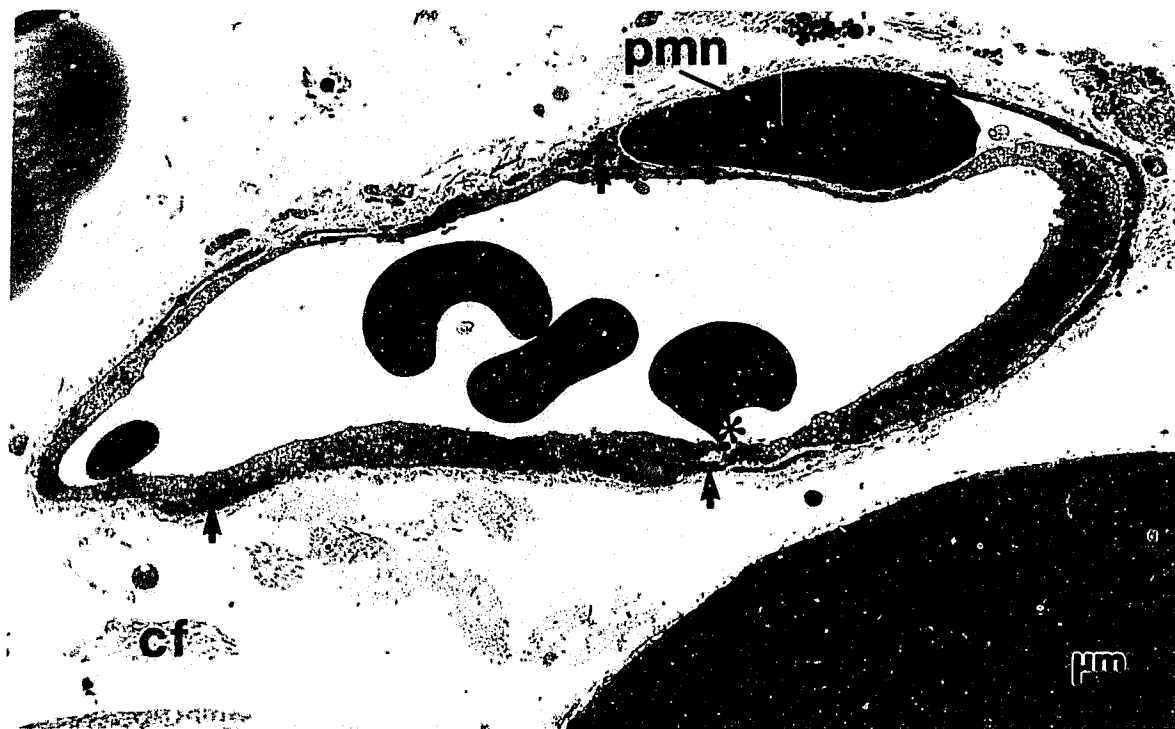


Fig. 17. Dermis venule showing pericyte coverage of Monastral Blue accumulations (↑), an endothelial cell gap (*) and a diapedesing polymorphonuclear leukocyte (pmn). An adipocyte (Ad) appears in the lower right. Collagen fibers are seen in the interstitium (cf). x 5,000.

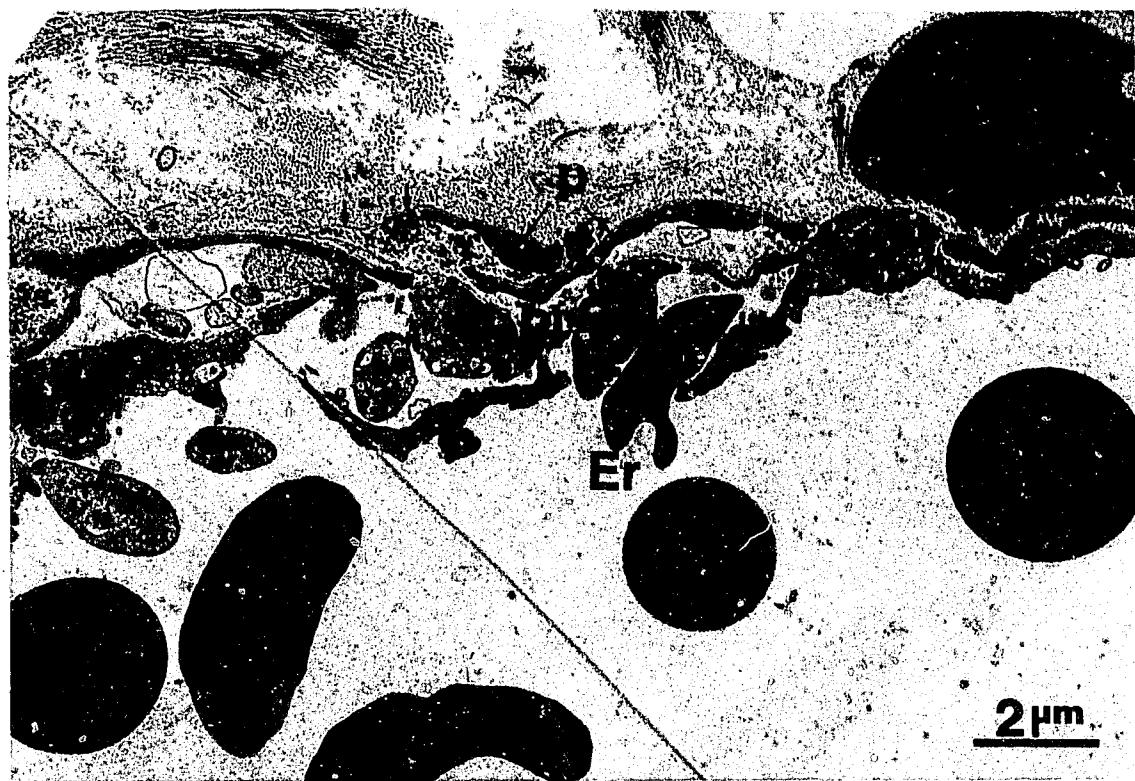


Fig. 18. Region of extensive gap formation in cremaster venule showing discontinuous endothelium (E), platelets (Pl) and extravasating erythrocytes (Er). Monastral Blue deposits are retained within the venule wall by both pericyte processes (p) and basement membrane (↓). Nuclear region of a pericyte appears at upper right. $\times 8,000$.

3.4 Discussion

Venules can be identified either by anatomical or physiological techniques. A physiological definition of venules, in this case the presence of endothelial cell gaps in response to histamine, was employed in this study. Venules were identified by the presence of the vascular label Monastral blue within the vessel wall. This method of identification is more reliable than older studies which rely on identifying vessels by their diameter. The latter method is becoming obsolete since vessel diameter can vary greatly within the same vascular bed due to techniques of sample preparation (e.g., fixation method or fixatives used), as well as due to organ specific or species specific variation (122). Anesthesia, surgical procedures and manipulative trauma can also alter blood flow, inhibit vasomotion and induce vasodilation, thus changing the vessel diameters (123).

Heltianu et al. (67) localized histamine H₂-receptors along endothelial cell junctions in mouse venules. When these receptors are activated endothelial separation occurs and a selective increase in macromolecular permeability is observed. This response is confined to post capillary venules (5,6,7). Utilizing Monastral blue is an excellent method for identifying venules because MB passes through endothelial gaps but does not cross the basement membrane and pericyte processes. It is incorporated within the vessel wall, making

venules easily visible with the naked eye, and in light and electron microscopy.

Interarterial perfusion of glutaraldehyde results in instantaneous fixation of the microvessels in rat mesentery, with accurate preservation of prefixation dimensions of the various segments of the vascular bed (122). In this study a total body vascular perfusion protocol, a modification of the one described by Rhodin (122), was employed to simultaneously fix all the tissues of the rat body at a physiological pressure and at a precise time so that different tissue samples could be taken from one animal for purposes of comparison. At all stages of tissue fixation the solutions used were adjusted to 350 mOsm, as suggested by Louw et al. (124). Vascular perfusion at physiological pressure enabled rapid fixation of the vascular structure and maintenance of vessel patency. The control tissue in this experiment did not show signs of increased permeability of the venules. Therefore, the experimental protocol i.e. surgery, anesthesia, perfusion was not regarded as contributing to the permeability seen in the histamine injection sites.

It has been well established that a maximal effect of mediators such as histamine, tachykinins, and leukotrienes is established within 3 to 10 minutes (7,97,125). Other workers have further established that the endothelial gaps that form in response to histamine begin at 4 minutes in cremaster muscle (49). The results of this study correlate well for

cremaster muscle. However venule gaps in dermal and tracheal tissue appear to have occurred earlier than 4 minutes and closed again by the time the tissues were fixed at 4 minutes. Very few gaps were found in dermis and trachea compared to cremaster muscle, although substantial Monastral blue accumulation was observed. This suggested that gap formation had taken place prior to the sampling time. This would agree with the work by MacDonald (126) who suggests the gaps that form in trachea venule endothelium in response to histamine occur at 2 minutes.

3.4.1 Morphology of the venule wall

The present study has documented the structural complexity of the pericyte-endothelial cell relationship of the venule wall in trachea, dermis and cremaster muscle during a histamine-induced increase in permeability. Although unlikely, there is a possibility that the results may not be representative of the total population of venules because the protocol selected for those venules responsive to histamine. The pericyte coverage of venules was found to be $82 \pm 12\%$ for trachea, $71 \pm 20\%$ for dermis and $85 \pm 18\%$ for cremaster muscle. Only coverage by first order pericytes, defined as the inner most layer, was measured, based upon the rationale that subsequent layers of pericytes were not apposed to, and, hence, could not directly interact with, endothelial cells.

Overlapping of pericyte processes is common in venules but not in capillaries (72).

Morphometric analysis of the pericyte-endothelial cell relationship has only previously been done on capillaries. One such study, done in skeletal and cardiac muscles, found that 22% of the circumference of skeletal muscle capillaries were enveloped by pericytes (92). A similar morphometric study of bovine gas exchange capillaries showed that average pericyte coverages were approximately 20% (Sims and Westfall, 1983). The increased coverage of venules by pericytes is consistent with previous non-quantitative observations by TEM (72) and SEM (127). The higher pericyte coverage of the venule wall suggests that the pericyte may have a functional role in the venule wall.

There was a significant difference between pericyte coverage of cremaster muscle ($85 \pm 18\%$) and dermal ($71 \pm 20\%$) venules. The lower percentage coverage of dermal venules suggest that the role of pericytes in this location, where vessels are already surrounded by an abundance of collagen, may not be structural support but rather a modulation of permeability.

There was no significant difference in the thickness of the venule wall in the three tissues.

3.4.2 Pericyte-endothelial cell relationships

Pericytes on the venules in cremaster muscle were found to be strategically located over histamine induced gaps. Pericyte processes formed a consistent covering over the gaps, often assuming a bridge-like appearance. The processes were completely surrounded by basement membrane. There was a random distribution of pericytes over endothelial cell gaps in both tracheal and dermal venules.

In both dermal and cremaster tissue, the orientation of pericytes on venules was not random. Instead there was a significant tendency for pericytes to overlay endothelial junctions. Endothelial gaps always occur at endothelial junctions (5) where mediator receptors are localized (67). Preferential locating of pericytes over junctions is consistent with the hypothesis that pericytes may modulate the leakage that occurs through gaps in response to inflammatory mediators.

In this report the pericyte is further implicated as a component of the venule wall that is crucial to its integrity. The consistent covering of endothelial gaps by pericytes in the cremaster muscle venules suggest a structural role as well. Gaps formed in response to mediators are quite large ($1 \mu\text{m}$). Yet the endothelial integrity is preserved during gap formation. The pericyte and basement membrane, in combination, effectively prevented the extravasation of red

blood cells, platelets and vascular labels, retaining them within the vascular wall, at least for the 4 minute duration of this study. This finding parallels the work by Rhodin and Fugita (89) who noticed a similar phenomenon in developing capillary sprouts. In that study pericytes were described as "umbrella" cells located over the leaky, immature, endothelial cell junctions.

The pericyte may also be essential for maintaining the structure of the vessel wall during diapedesis. Polymorphonuclear leukocytes (PMNS) leave the circulation through post capillary venules via endothelial junctions (114). The present study demonstrated pericytes were localized over junctions in both dermis and cremaster. Therefore it is interesting to speculate that they may be holding the venule wall together while PMNS migrate through to the interstitium. Diapedesis is not accompanied by an increased vascular leakage (128). Hurley (129) also showed that although emigrating leukocytes may not cause leaks in the endothelium, they temporarily tear apart the basement membrane surrounding the vessel wall. He demonstrated this by infusing intravascularly the vascular label India ink immediately after injecting histamine in the skin. The area of skin injected had received an injection of serum 4 hours previously to induce diapedesis. The post diapedesis vessels spilled their carbon out into the tissue spaces through the holes created by escaping leukocytes. Since the basement membrane continuity

was obviously disrupted, the pericyte could be functioning as the sole source of vessel wall support during this process.

In conclusion, as roles of pericytes in vitro and in vivo are further characterized, their implications in health and disease will become more apparent. The data presented here are consistent with proposed roles that pericytes control macromolecular and cellular movement across the venule wall in vivo and protect the integrity of the wall during mediator-induced vascular permeability.

4. GENERAL SUMMARY AND DISCUSSION

The study of inflammation is an important concern in both human and veterinary medicine. The acute inflammatory response, is comprised of a complex series of events that lead to both functional and morphological changes in the blood vessels.

Typical vascular changes are as follows: immediately following injury there is a transient constriction of local arterioles followed shortly thereafter by dilatation of all the small blood vessels in the area. As a result, the blood flow to the area increases as much as ten-fold and then returns to normal. While the blood vessels are dilated there is also an increase in their permeability and protein-rich plasma exudes into the tissues where it causes local edema and swelling.

Within a few hours of the onset of the vascular changes, leukocytes (neutrophils, eosinophils and monocytes) adhere to the vascular endothelium, a process called pavementing. If the blood vessels are damaged, platelets may also adhere and release vasoactive and clotting substances.

After adhering to the venule walls, the leukocytes migrate into the surrounding tissue via the junctions between endothelial cells. Neutrophils and eosinophils will be the first to arrive in inflamed tissues, followed later by the monocytes. Once within tissues, the cells are attracted by

chemotactic factors to sites of bacterial growth or tissue damage. There they proceed to phagocytose and destroy any foreign material and, and in the case of monocytes, remove dead and dying tissue.

The venule thus appears to be the primary vascular component of the pathophysiological changes in acute inflammation since the increased permeability in response to inflammatory mediators and the diapedesis of leukocytes is known to occur exclusively from venules (56,114).

The venule wall is composed of endothelial cells, pericytes and their basal laminae. Although the pericyte is an integral component of the venule and is also found in highest concentration on this segment of the microvasculature, investigations into the pericyte endothelial-cell relationship during an acute inflammatory response and possible roles for pericytes are lacking.

In this thesis, the ultrastructure of the venule wall was investigated to quantitate the pericyte-endothelial cell relationship. Previous work quantitating pericytes has been restricted to capillaries (82,91,92,93,94). Data presented in this thesis indicated that the pericyte and its basement membrane may also have a role in histamine-induced vascular permeability in venules.

The local injection of vasoactive mediators, such as histamine, is a simple model of increased vascular permeability (130). Injection of histamine in an appropriate

dose into skin or muscle causes a massive but short lived increase in vascular permeability. Leakage of plasma proteins begins immediately after a histamine injection, rises rapidly to a maximum and ceases abruptly 10-15 minutes later. This type of increased permeability is not followed by any permanent change in either structure or reactivity of the leaking vessels.

The structural basis of histamine-induced leakage was first described by Majno and Palade (4). After examining the effects of serotonin and bradykinin on the small blood vessels of skeletal muscles, they reported that these agents cause transient openings, $0.1 - 0.4 \mu\text{m}$ in diameter, to form in the endothelium of venules. There is no evidence for concurrent damage to endothelial cell cytoplasm. When leakage ceases, the gaps close, leaving a morphologically normal endothelium. It is now generally accepted that active contraction of the endothelial cell is the most plausible mechanism underlying gap-formation under the influence of vasoactive mediators (58). It has also been demonstrated that receptors for vasoactive mediators are located in concentrated regions along the endothelial cell junctions in venules (67). Fox et al. (47) made a three-dimensional computer-assisted reconstruction of the walls of vessels stimulated by histamine. Every gap which they examined was found to lie within an intercellular junction.

Majno and Palade (4) located their transient sites of

leakage by injecting marker particles of colloidal carbon or mercuric sulphide intravenously before applying the vasoactive substance. When gaps form in the vascular endothelium, plasma and circulating marker particles are forced out through the gaps by intravascular hydrostatic pressure. The plasma passes through the basement membrane but carbon and mercuric sulfide particles are too large to do likewise and accumulate against the vascular basement membrane. The marker particles in circulating blood are removed within 30-60 minutes by phagocytic cells in the liver and spleen, but particles trapped between vascular endothelium and the basement membrane remain in that position for many hours, or even days - long after the gap in the underlying endothelium has closed. Such labeled vessels can be readily detected in both histological and cleared specimens of the injured area. This is the basis of the vascular labeling technique (96). Since colloidal carbon and mercuric sulfide are no longer commercially available, Monastral Blue was used as the vascular label in this study. A re-evaluation of MB's properties prompted by discrepancies in the literature, revealed that MB is removed from the vascular system within 7-10 minutes of an intravenous infusion. It also caused a significant decrease, $30 \pm 13\%$, in the arterial blood pressure. Thus there are some limitations to the use of MB in vivo.

The combined use of vascular labeling and electron microscopy is a much more sensitive way of detecting the

presence of defects in vascular endothelium than is unaided electron microscopy. The amount of tissue that can be examined by electron microscopy is so small that it is impractical to find gaps without the use of a vascular label. However, even very small deposits of MB can be detected by careful examination of fresh or cleared specimens, and if subsequent electron microscopic studies are made of MB labeled areas, it is relatively easy to find whether the MB lies over the vascular endothelium in the vessel wall. If intramural MB deposits are found, this is conclusive evidence that gaps are, or have been, present as MB particles are too large to escape through either continuous or fenestrated endothelium in any other known way.

An experimental model which would enable ultrastructural comparison of different tissues from one animal, fixed at a precise time and with positive identification of venules has not been previously used to study pericyte-endothelial cell relationships. Such a model was developed by combining techniques of intraarterial vascular perfusion at in vivo vascular pressure with a MB vascular labeling technique. Unlike other models of inflammation such as the hamster cheek pouch and cremaster muscle models, an intraarterial vascular perfusion model is less traumatic (i.e. vessels are not disturbed by manipulation). Thus there is less physical artifact and one can study more than one tissue concurrently.

Electron microscopic and morphometric techniques employed

in this study revealed there is a much higher coverage of venule by pericytes in trachea ($82 \pm 12\%$), dermis ($71 \pm 20\%$) and cremaster muscle ($85 \pm 18\%$) than what has previously been reported in morphometric studies of capillaries, where values reported are in the 15-25% range (82,91,92,93,94). The non-random distribution of pericytes over endothelial cell junctions in dermal and cremaster muscle indicated a specific functional relationship between pericytes and the endothelium, possibly in the modulation of vascular leakage.

Leukocytes always leave the circulation through post-capillary venules via endothelial cell junctions (114). It has been widely assumed that the venule wall plays a purely passive role during the escape of leukocytes. However, diapedesis is not accompanied by an increased vascular permeability (129,131). An effective "protein seal" appears to be maintained in vivo between endothelial cells and emigrating leukocytes at all stages of their escape. While most investigations have presumed that endothelial cells produce this seal, pericytes are equally plausible, based on their structure and positioning. Pericyte concentration over endothelial cell junctions, their many contacts with the endothelium and their tonic contractile properties suggest that they may have a role in maintaining the vessel integrity during diapedesis.

Pericytes in cremaster muscle venules are strategically located over the endothelial gaps formed in response to

histamine. Their consistent bridge-like covering of gaps prevented the extravasation of vascular label, red blood cells and platelets. Pericytes appeared to maintain the integrity of the vessel wall during gap formation by holding the endothelium together.

In contrast to the other tissues studied, the venules of the tracheal microcirculation showed a random distribution of pericytes over both endothelial junctions and gaps. This finding implies that in this tissue pericytes are not specifically involved with vascular leakage. Inflammatory extravasation of protein-rich plasma into the interstitium through mediator-induced gaps in the endothelium generates airway submucosal and mucosal edema (115,116). This edema is a feature of asthmatic airways and it is interesting to speculate that the lack of pericyte-endothelial junction and gap coverage in these vessels may be contributing to the marked increase in permeability of these vessels.

Various peripheral vascular disease conditions involve alterations of the venules. These include, to name a few, low-flow states, circulatory shock, hypertension, diabetes mellitus, progressive systemic sclerosis (scleroderma) psoriasis and asthma (132). The possibility of quantitating the in vivo structure-activity relationships for vasoactive mediators at the microcirculatory level in different types of venules, as well as further elucidating the cellular interactions involved, may lead to the design of new drugs for

the treatment of these conditions.

Research during the past decade has just begun to suggest functions of pericytes in the microvasculature, although many questions remain to be answered before the precise roles of pericytes are known. Areas of future research include studies of:

- 1) the relationship of pericytes to endothelial junctions that have been labeled for mediator receptors,
- 2) three-dimensional analysis of the pericyte-endothelial cell gap relationship through serial section reconstruction,
- 3) pericyte relationship to endothelium in response to mediators other than histamine, such as platelet activating factor, neuropeptides and leukotrienes,
- 4) species and organ-specific properties of pericytes,
- 5) the precise nature of the pericyte and endothelial basal laminae and differences between them, if any,
- 6) the contractile nature of pericytes in vitro and in vivo, and
- 7) possible junctional communication between pericytes and between pericytes and endothelial cells.

The paucity of information concerning the characterization of pericytes is due largely to the inaccessibility of the cell in vivo and to the lack of methods for their isolation and culture. Studies addressing the function and origin of pericytes have been further hampered

by the lack of a definitive cell marker. Techniques for culturing pericytes have improved considerably in the past few years (133,134). These improved methods for culturing pericytes both alone and congruently with endothelial cells will allow improved functional studies of pericytes. Recently specific markers for pericytes such as the monoclonal antibody anti- α -sm-1 (73) and a cell surface protein designated PC4 (135) have been discovered. Improved methods for the study of pericytes will lend to further elucidation of exact roles of pericytes in the venule wall

REFERENCES

1. RYAN GB, MAJNO G. Historic Highlights. In: Thomas BA Ed. Inflammation. Kalamazoo: The Upjohn Company, 1977: 6.
2. HURLEY JV. The cardinal signs of inflammation. In: Acute Inflammation. New York: Churchill Livingstone; 1983: 3
3. MOVAT HZ. Historical survey. In: The Inflammatory Reaction. New York: Elsevier; 1985: 2-5
4. MAJNO G, PALADE GE. Studies on inflammation I. The effects of histamine and serotonin on vascular permeability: An electron microscopic study. *J Biophys Biochem Cytol* 1961; 11: 571-603.
5. MAJNO G, PALADE GE, SCHOEFL GI. Studies on inflammation II. The site of action of histamine and serotonin along the vascular tree: A topographic study. *J Biophys Biochem Cytol* 1961; 11: 607-626.
6. MAJNO G, GILMORE V, LEVENTHAL M. On the mechanism of vascular leakage caused by histamine-type mediators. A microscopic study in vivo. *Circ Res* 1967; 21: 833-847.
7. MAJNO G, SHEA SM, LEVENTHAL M. Endothelial contraction induced by histamine-type mediators. An electron microscopic study. *J Cell Biol* 1969; 42: 647-672.
8. WILHELM DL. Chemical mediators. In: Zweitach BW, Grant C and McClusky RT, eds. The inflammatory Process. 2nd Ed. New York: Academic Press, 1973: 251-301.
9. THEOHARIDES TC, BORDY PK, TSAKALUS ND, ASKENASE PW. Differential release of serotonin and histamine from mast cells. *Nature* 1982; 297: 229-231.
10. ROWLEY DA, BENDITT EP. 5-Hydroxytryptamine and histamine as mediators of vascular injury produced by agents which damage mast cells in rats. *J Exp Med* 1956; 103: 399-412.
11. MOVAT HZ, MACMORINE DRL, TAKEUCHI Y. The role of PMN-leukocyte lysosomes in tissue injury, inflammation and hypersensitivity. III. Mode of action and properties of vascular permeability factors during in vitro phagocytosis. *Int Arch Allergy Appl Immunol* 1971; 40: 218-235.

12. PETERS SP, SIEGEL MI, KAGER-SOBOTKA A, LICHTENSTEIN LM. Lipoxygenase products modulate histamine release in human basophils. *Nature* 1981; 292: 455-457.
13. TURNER SR, CAMPBELL JA, LYNN WS. Polymorphonuclear chemotaxis toward oxidized lipid components of cell membrane. *J Exp Med* 1975; 141: 1437-1441.
14. DAHLEN SE, BJORK J, HEDQUIST P, ARFORSS KE, HAMMARSTROM S, LINDGREN JA, SAMUELSON B. Leukotrienes promote plasma leakage and leukocyte adhesion in postcapillary venules. In vivo effects with relevance to the acute inflammatory response. *Proc Natl Acad Sci* 1981; 78: 3887-3891.
15. SOTER NA, LEWIS RA, COREY EJ, AUSTEN KF. Local effects of synthetic leukotrienes (LTC₄, LTD₄, LTE₄, and LTB₄) in human skin. *J Invest Dermatol* 1983; 80: 115-119.
16. JORIS I, MAJNO G, COREY EJ, LEWIS RA. The mechanism of vascular leakage induced by leukotriene E₄. *Am J Pathol* 1987; 126: 19-24.
17. MOVAT HZ, RETTL C, BURROWES CE, JOHNSON MG. The in vivo effects of leukotrienne B₄ on polymorphonuclear leukocyte and the microcirculation. Comparison with activated complement (C5a des Arg) and enhancement by prostaglandin E₂. *Am J Pathol* 1984; 115: 233-244.
18. WILLIAMS TJ, MORLEY J. Prostaglandins as potentiators of increased vascular permeability of inflammation. *Nature* 1973; 246: 215-217.
19. JOHNSTON MG, HAY JB, MOVAT HZ. Potential role of prostaglandins in modulating vascular permeability changes during inflammation through local alterations in blood flow (hyperemia). In: Grayson J and King W, eds. *Microcirculation, Vol. 2: Transport Mechanisms and Disease States*. New York: Plenum Press, 1975: 227-229.
20. JOHNSTON MG, HAY JB, MOVAT HZ. The modulation of enhanced vascular permeability by prostaglandins through alterations in blood flow (hyperemia). *Agents Actions* 1976; 6: 707-711.
21. ISSEKUTZ AC. Effect of vasoactive agents on polymorphonuclear leukocyte emigration in vivo. *Lab Invest* 1981; 45: 234-240.

22. ISSEKUTZ AC, MOVAT HZ. The effect of vasodilator prostaglandins on polymorphonuclear leukocyte infiltration and vascular injury. *Amer J Pathol* 1982; 107: 300-309.
23. GOETZL E. Oxygenation products of arachidonic acid as mediators of hypersensitivity and inflammation. *Med Clin NA* 1981; 65: 809-828.
24. O'FLAHERTY, JT. Biology of disease: lipid mediators of inflammation and allergy. *Lab Invest* 1982; 47: 314-329.
25. BENVENISTE J. Platelet-activating factor, a new mediator of anaphylaxis and immune complex deposition from rabbit and human basophils. *Nature* 1974; 249: 581-584.
26. HAMASASKI Y, MOJARAD M, SAGA T, TAI H, SAID SI. Platelet activating factor raises airway and vascular pressures and induces edema in lungs perfused with platelet free solution. *Am Rev Respir Dis* 1984; 129: 742-746.
27. O'DONNELL SR, BARNETT CJK. Microvascular leakage to platelet activating factor in guinea pig trachea and bronchi. *Eur J Pharmacol* 1987; 138: 385-396.
28. PETTIPHER ER, HIGGS GA, HENDERSON B. Interleukin-1 induces leukocyte infiltration and cartilage proteoglycan degradation in the synovial joint. *Proc Natl Acad Sci* 1986; 83: 8749-8753.
29. GREAVES MW. Inflammation and mediators. *Br J Derm* 1988; 119: 419-426.
30. WILHELM DL. Kinins in human disease. *Annu Rev Med* 1971; 22: 63-64.
31. YAMAMOTO T. In: Cohen S, Hayashi H, Saito K and Takada A, eds. *Chemical Mediators of Inflammation*. Tokyo: Academic Press, 1985.
32. REGOLI D, BARABE J. Pharmacology of bradykinin and related kinins. *Pharm Rev* 1980; 32: 1-46.
33. COCHRAN CG, GRIFFIN JH. The biochemistry and pathophysiology of the contact system of plasma. *Adv Immunol* 1982; 33: 241-306.

34. SUGIO K, GREENBAUM LM. Increase in vascular permeability of rat and guinea pig skin by T-Kinin. *Inflam* 1988; 12: 407-412.
35. SALDEEN T. The microembolism syndrome: a review. In: Saldeen T, Almquist T and Wiksell, eds. *The Microembolism Syndrome*. Philadelphia, PA: Current Books, 1979.
36. WARD PA. Complement derived leukotactic factors in pathological fluids. *J Exp Med* 1971; 134: 1095-1135.
37. WIGGINS RC, GIGLAS PC, HENSON PM. Chemotactic activity generated from the fifth component of complement by plasma killikriens of the rabbit. *J Exp Med* 1981; 153: 1391-1404.
38. SAID S. Vasoactive peptides in the lung with special reference to vasoactive intestinal peptide. *Exp Lung Res* 1982; 3: 343-348.
39. BARNES PJ. Vasoactive intestinal peptide and pulmonary function. In: Hollinger MA, Ed. *Current Topics in Pulmonary Pharmacology and Toxicology*. Philadelphia: Praeger Scientific, 1987.
40. FULLER RW, MAXWELL DL, DIXON CMS, MCGREGOR GP, BARNES VF, BLOOM SR, BARNES PJ. The effects of substance P on cardiovascular and respiratory function in subjects. *J Appl Physiol* 1987; 62: 1477-1479.
41. FOREMAN JC. Neuropeptides and the pathogenesis of allergy. *Allergy* 1987; 42: 1-11.
42. BARNES PJ. Neuropeptides and airway smooth muscle. *Pharmac Ther* 1988; 36: 119-129.
43. BRAIN SD, WILLIAMS TJ. Inflammatory edema induced by synergism between calcitonin gene-related peptide (CGRP) and mediators of increased vascular permeability. *Br J Pharmac* 1985; 86: 855-860.
44. BRAIN SD, TIPPING JR, MORRIS HR, MACINTRE I, WILLIAMS JJ. The potent vasodilator activity of calcitonin gene-related peptide in human skin. *J Invest Derm* 1986; 87: 533-536.
45. LUNDBERG JM, TERENIUS L, HOKFELT T, MARTLING LR, TATEMOTO K, MUTT V, POLAK J, BLOOM S AND GOLSTEIN M. Neuropeptide Y (NPY)-like immunoreactivity in peripheral nonadrenergic neurons and effects of NPY on sympathetic function. *Act Physiol Scand* 1982; 116: 477-480.

46. LARSON GL, HENSON PM. Mediators of inflammation. *Ann Rev Immunol* 1983; 1: 335-359.
47. FOX J, GALLY F, WAYLAND H. Action of histamine on the mesenteric microvasculature. *Microvasc Res* 1980; 19: 108-126.
48. GREGA GJ, SVENSJO E. Pharmacology of water and macromolecular permeability in the forelimb of the dog. In: Staub NC and Taylor AE, eds. *Edema*. New York: Raven Press, 1984: 405-425.
49. MILLER FN, JOSHUA IG, ANDERSON GL. Quantitation of vasodilator-induced macromolecular leakage by *in vivo* fluorescent microscopy. *Microvasc Res* 1982; 24: 56-67.
50. SVENSJO E. Bradykinin and Prostaglandin E₁, E₂ and F₂-induced macromolecular leakage in the hamster cheek pouch. *Prostaglandins Med* 1978; 1: 379-410.
51. SVENSJO E, ADAMSKI SW, SU K, GREGA GJ. Quantitative physiological and morphological aspects of microvascular permeability changes induced by histamine and inhibited by terbutaline. *Acta Physiol Scand* 1982; 116: 265-273.
52. GABBIANI G, BADONNEL MC, MAJNO G. Intra-arterial injection of histamine, serotonin or bradykinin: A topographic study of vascular leakage. *Proc Soc Exp Biol* 1970; 135: 447-452.
53. HURLEY JV, MCQUEEN A. The response of the fenestrated vessels of the small intestine of rats to application of mustard oil. *J Path* 1971; 105: 21-29.
54. PIETRA GG, SZIDON JP, LEVENTHAL MM, FISHMAN AP. Anatomic basis of histamine-mediated peribronchial interstitial edema. *Lab Invest* 1970; 22: 507-508.
55. CUNNINGHAM AL, HURLEY JV. Alpha-naphthyl-thiourea-induced pulmonary oedema in the rat: A topographical and electron-microscope study. *J Pathol* 1972; 106: 25-35.
56. PALADE GE, SIMIONESCU M and SIMIONESCU N. Structural aspects of the permeability of the microvascular endothelium. *Acta Physiol Scand Suppl* 1979; 463: 11-32.
57. SVENSJO E, GREGA GJ. Evidence for endothelial cell-mediated regulation of macromolecular permeability by postcapillary venules. *Fed Proc* 1986; 45: 89-95.

58. RAGAN DMS, SCHMIDT EE, MACDONALD IC, GROOM AC. Spontaneous cyclic contractions of the capillary wall in vivo. Impeding red cell flow: A quantitative analysis-evidence for endothelial contractility. *Microvasc Res* 1988; 36: 13-30.
59. JOYNER WL, SVENSSJO E, ARFORSS KE. Simultaneous measurements of macromolecular leakage and arteriolar blood flow as altered by PGE₂ and B₂ stimulation in the hamster cheek pouch. *Microvasc Res* 1979; 18: 301-310.
60. CRONE C. Modulation of solute permeability in microvascular endothelium. *Fed Proc* 1986; 45: 77-83.
61. JORIS I, MAJNO G, RYAN GB. Endothelial contraction in vivo: A study of the rat mesentery. *Virchows Arch B* 1972; 12: 73-83.
62. KILLACKEY JF, JOHNSTON MG, MOVAT HZ. Increased permeability of microcarrier-cultured endothelial monolayer in response to histamine and thrombin A. A model for the study of increased vasopermeability. *Am J Path* 1986; 122: 50-61.
63. DECLERK F, DEBRABANDER M, NEELS H, VANDEVELDF V. Direct evidence for the contractile capacity of endothelial cells. *Thromb Res* 1981; 23: 505-520.
64. BECKER CG, NACHMAN RL. Contractile proteins of endothelial cells, platelets and smooth muscle. *Am J Pathol* 1973; 71: 1-22.
65. DRENCKHAHN DL. Cell motility and cytoplasmic filaments in vascular endothelium. *Prog Appl Microcirc* 1983; 1: 53-70.
66. DRENCKHAHN D, WAGNER J. Stress fibers in the splenic sinus endothelium in situ: Molecular structure, relationship to the extracellular matrix and contractility. *J Cell Bio* 1986; 102: 1738-1747.
67. HELTIANU C, SIMIONESCU M, SIMIONESCU N. Histamine receptors of the microvascular endothelium revealed in situ with histamine-ferritin conjugate: Characteristic high affinity binding sites in venules. *J Cell Biol* 1982; 93: 357-364.
68. BUNGAARD M. The three-dimensional organization of tight junctions in a capillary endothelium revealed by serial-section electron microscopy. *J Ultrastructure Res* 1984; 88: 1-17.

69. LIDDELL RHA, SCOTT ARW, SIMPSON JG. Histamine-induced changes in the endothelium of post capillary venules: effects of chelating agents and cytochalasin B. In: *Biblthca Anat*, Vol 20. Karger: Basal, 1981: 109-112.
70. GREGA GJ, ADAMSKI SW, SVENSJO E: Is there evidence of venular large junctional gap formation in Inflammation? *Microcirc Endoth Lymph* 1985; 2: 211-234.
71. SIMS DE. The pericyte - a review. *Tissue Cell* 1986; 18: 152-174.
72. RHODIN JAG. Ultrastructure of mammalian venous capillaries, venules and small collecting veins. *J Ultrastructure Res* 1968; 25: 452-500.
73. SKALLI O, PELTE MF, PECLET MC, GABBIANI G, GUGLIOTTA P, BUSSOLATI G, RAVAZZOLA M, ORCI L. α -Smooth muscle actin, a differentiation marker of smooth muscle cells is present in microfilamentous bundles of pericyte. *J Histochem Cytochem* 1989; 37: 315-321.
74. MEYRICK B, FUJIWARA K, REID L. Smooth muscle myosin in precursor and mature smooth muscle cells in normal pulmonary arteries, and the effect of hypoxia. *Exp Lung Res* 1981; 2: 303-313.
75. JOYCE NC, HAIRE MF, PALADE GE. Contractile proteins in pericytes II. Immunohistochemical evidence of the presence of two isomyosins in graded concentrations. *J Cell Biol* 1985; 100: 1387-1395.
76. JOYCE NC, DELAMILLI P, BOYLES J. Pericytes, like vascular smooth muscle cells, are immunocytochemically positive for cyclic GMP-dependent protein kinase. *Microvasc Res* 1984; 28: 206-219.
77. FUJIMOTO T, SINGER SJ. Immunocytochemical studies of Desmin and Vimentin in Pericapillary Cells of Chickens. *J Histochem Cytochem* 1987; 35: 1105-1115.
78. KELLEY C, D'AMORE PD, HECHTMAN HB, SHEPRO D. Microvascular pericyte contractility in vivo: Comparison with other cells of the vascular wall. *J Cell Biol* 1987; 104: 483-490.
79. COHEN MP, FRANK RN, KHALIFA AA. Collagen production by cultured retinal capillary pericytes. *Invest Ophthal Vis Sci* 1980; 19: 90-94.

80. MILLER FN, SIMS DE. Contractile elements in the regulation of macromolecular permeability. *Fed Proc* 1986; 45: 84-88.
81. SIMIONESCU N, SIMIONESCU M, PALADE G. Structural basis of permeability in sequential segments of the microvasculature of the diaphragm II. Pathways followed by microperoxidase across the endothelium. *Microvasc Res* 1978; 15: 17-36.
82. SIMS DE, WESTFALL JA. Analysis of the relationship between pericytes and gas exchange capillaries in neonatal and mature bovine lungs. *Microvasc Res* 1983; 25: 333-342.
83. MATSUSAKA T. Ultrastructural differences between the choriocapillaris and retinal capillaries on the human eye. *Jap J Ophthal* 1970; 14: 58-71.
84. IMAYAMA S, URABE T. Pericytes on the dermal microvasculature of the rat skin. *Anat Embryol* 1984; 169: 271-274.
85. HULSTROM D, SVENSSJO E. Intravital and electron microscopic study of bradykinin induced vascular permeability changes using FITC-dextran as a tracer. *J Pathol* 1985; 29: 125-133.
86. COTRAN RS, MAJNO G. The delayed and prolonged vascular leakage in inflammation I. Topography of the leaking vessels after thermal injury. *Am J Pathol* 1964; 45: 261-281.
87. COTRAN RS. The delayed and prolonged vascular leakage in inflammation II. An electron microscopic study of the vascular response after thermal injury. *Am J Pathol* 1965; 46: 589-620.
88. JORIS I, DEGIROLAMI U, WORTHHAM K, MAJNO G. Vascular labeling with Monastral blue B. *Stain Technol* 1982; 57: 177-83.
89. RHODIN JAG and FUGITA H. Capillary growth in the mesentary of normal young rats. Intravital video and electron microscope analyses. *J Submicrosc Cytol Pathol* 1989; 21: 1-34.
90. SZABO S. Role of sulphhydryls and early vascular lesions in gastric mucosal injury. *Acta Physiol Hung* 1984; 64: 203-214.

91. TILTON RG, KILO C, WILLIAMSON JR. Pericyte-endothelial relationships in cardiac and skeletal muscle capillaries. *Microvasc Res* 1979; 18: 336-352.
92. TILTON RG, KILO C, WILLIAMSON JR, MARCH DW. Differences in pericyte contractile function in rat cardiac and skeletal muscle microvasculatures. *Microvasc Res* 1979; 18: 336-352.
93. HO KL. Ultrastructure of cerebellar capillary hemangioblastoma IV. Pericytes and their relationship to endothelial cells. *Acta Neuropathol.* 1985; 67: 254-264.
94. WILLIAMSON JR, TILTON RG, KILO O, SIMON Y. Immunofluorescent imaging of capillaries and pericytes in human skeletal muscle and retina. *Microvasc Res* 1980; 20: 233-241.
95. COTRAN RS, LABATTUTA M, MAJNO G. Studies on inflammation: fate of intramural vascular deposits induced by histamine. *Am J Pathol* 1965; 47: 1045-1077.
96. COTRAN RS, SUTER ER, MAJNO G. The use of colloidal carbon as a tracer for vascular injury. A review. *Vasc Dis* 1967; 4: 107-27.
97. PIETRA GG, SZIDON JP, LEVENTHAL MM, FISHMAN AP. Histamine and interstitial pulmonary edema in the dog. *Circ Res* 1971; 29: 323-337.
98. HURLEY JV. Current views on the mechanism of pulmonary edema. *J Pathol* 1978; 125: 59-79.
99. TAKAGI T, FORREST MJ, BROOKS PM. A pharmacological and histological examination of the microcirculation of the rat subcutaneous air-pouch: microcirculation of the rat air-pouch. *Pathol* 1987; 19: 294-298.
100. MCDONALD DM, MITCHELL RA, GABELLA G, HASKALL A. Neurogenic inflammation in the rat trachea II. Identity and distribution of nerves mediating the increase in vascular permeability. *J Neurocytol* 1988; 17: 605-628.
101. ALBERTINE KH, STAUB NC. Vascular tracers alter hemodynamics and airway pressure in anesthetized sheep. *Microvasc Res* 1986; 32: 279-288.
102. CANADIAN COUNCIL ON ANIMAL CARE. Guide to the Care and Use of Experimental Animals, Vols 1&2, 1980. Ottawa.

103. FLYNN SB, OWEN DAA. Histamine receptors in peripheral vascular beds in the cat. *Br J Pharmac* 1975; 55: 181-188.
104. BLACK JW, OWEN DAA, PARSONS ME. An analysis of the depressor responses to histamine in the cat and dog: involvement of both H_1 - and H_2 - receptors. *Br J Pharmac* 1975; 54: 319-324.
105. FREEDMAN FB, JOHNSON JA. Equilibrium and kinetic properties of the Evans blue-albumin system. *Am J Physiol* 1969; 216: 675-681.
106. LEVIK JR, MICHEL CC. The permeability of individually perfused frog mesenteric capillaries to T-1824 and T-1824-albumin as evidence for a large pore system. *Quart J Exp Physiol* 1973; 58: 67-85.
107. HALPERN BN, BENECERRAF B, BIOZZI G. Quantitative study of the granulopectic activity of the reticulo-endothelial system I. The effect of the ingredients present in India ink and of substances affecting blood clotting *in vivo* on the fate of carbon particles administered intravenously in rats, mice and rabbits. *Br J Exp Pathol* 1965; 34: 426-440.
108. COTRAN RS, MAJNO G. A light and electron-microscopic analysis of vascular injury. *Ann NY Acad Sci* 1964; 116: 750-763.
109. KRISTENSSON K, OLSSON Y. Accumulation of protein tracers in pericytes of the central nervous system following systemic injection in immature mice. *Acta Neurol Scand* 1973; 49: 189-194.
110. AUSPRUN KDH, FOLKMAN J. Migration and proliferation of endothelial cells in preformed and newly formed blood vessels during tumor angiogenesis. *Microvasc Res* 1977; 14: 53-65.
111. CROCKER DJ, MURAD TM, GEER JC. Role of the pericyte in wound healing. An ultrastructural study. *Exp Mol Pathol* 1970; 13: 51-65.
112. ORLIDGE A, D'AMORE PA. Inhibition of capillary endothelial cell growth by pericytes and smooth muscle cells. *J Cell Biol* 1987; 105: 1455-1462.
113. MAJNO G. Ultrastructure of the vascular membrane. In: *Handbook of Physiology*, Section 2, Vol III. Washington D.C.: American Physiological Society, 1965: 23-39.

114. MARCHESI VT, FLOREY TW. Electron microscopic observations on the emigration of leukocytes. Quart J Exp Physiol; 45: 343-348.
115. PERSSON CGA. Plasma Exudation and Asthma. Lung 1988; 166: 1-23.
116. O'DONNELL S. Airway microvascular permeability in asthma: A target for drug action? In: New anti-asthma drugs. Basal: Birkhauser Verlag, 1988, p.217-238.
117. SATO T. A modified method for lead staining of thin sections. J Electron Microscopy 1967; 16: 133-135.
118. WEIBEL ER. Stereological Methods Vol.1 Practical Methods for Biological Morphometry. New York: Academic Press 1979, p.31-37,204-210.
119. SAS INSTITUTE INC. SAS/STAT Guide for Personal Computers Version 6 Edition. Cary, NC: SAS Institute Inc., 1985: 1378
120. KLEINBAUM DG, KUPPER LL, MULLER KE. Applied Regression Analysis and other Multivariable Methods. 2nd ed. Boston: PWS - KENT Publishing Co., 1988.
121. STEEL RG, TORRIE JH. Principles and Procedures of Statistics-A Biometrical Approach. 2nd Ed. New York: McGraw-Hill Book Co. 1985, p.478.
122. RHODIN JAG. Perfusion and superfusion fixation effects on rat mesentary microvascular beds. Intravital and electron microscopic analyses. J Submicrosc Cytol 1986; 18: 453-470.
123. WEIDEMAN CA, SLAAF DW. A new skeletal muscle preparation for the study of microvascular function in intact unanesthetized animals. Microvasc Res 1987; 33: 413-416.
124. LOUW J, WOLFE-COOTE SA, DAY RS. Observations on the effects on tissue dimensions of altering osmium tetroxide molarity with sucrose and sodium chloride. J Electron Microsc Tech 1986; 4: 65-67.
125. PERSSON CGA, SVENSJO E. Vascular responses and their suppression: drugs interfering with venular permeability. In: Bonta IL, Bray MA, Parnham MJ (eds) Handbook of Inflammation, Vol 5. The Pharmacology of Inflammation. Amsterdam: Elsevier 1985: 61-81.

126. MCDONALD, DM. Neurogenic inflammation in the rat trachea. I. Changes in venules, leucocytes and epithelial cells. *J Neurocytol* 1988; 17: 583-604.
127. FUJIWARA T, UREHARA Y. The cytoarchitecture of the wall and the innervation pattern of the microvessels in the rat mammary gland: a scanning electron microscopic observation. *Am J Anat* 1984; 170: 39-54.
128. HURLEY JV. An electron microscopic study of leukocytic emigration and increased vascular permeability in rat skin. *Aust J Exp Biol Med Sci* 1963; 41: 171-186.
129. HURLEY . Acute inflammation: The effect of concurrent leukocytic emigration and increased vascular permeability on particle retention by the vessel wall. *Br J Exp Path* 1964; 45: 627-633.
130. HURLF JV. Increased vascular permeability 1. The nature of inflammatory exudate and the response to histone-type permeability factors. In: *Acute Inflammation*. New York: Churchill Livingstone, 1983: 30-
131. McQUEEN A, HURLEY JV. Aspects of increased vascular permeability following the intradermal injection of histone in the rat. *Pathol* 1971; 3: 191-202.
132. ALT BM. Pharmacology of venules: Some current concepts and clinical potential. *J Cardiovasc Pharm* 1983; 3: 1413-1428.
133. GITLIN JD, D'AMORE PA. Culture of retinal capillary cells using selective growth media. *Microvasc Res* 1983; 26: 74-80.
134. HERMAN IM, D'AMORE PA. Microvascular pericytes contain muscle and non-muscle actins. *J Cell Biol* 1985; 101: 43-52.
135. RISAU WR, SWEET E, D'AMORE PA. Preferential Expression of 130,000-Da Cell Surface Protein by Vascular Wall Cells in vitro and in vivo. *Microvasc Res* 1988; 35: 265-277.